Medical University of Graz

METABOLISM-SECRETION COUPLING AND MITOCHONDRIAL CALCIUM ACTIVITIES IN PANCREATIC BETA-CELLS

LUKAS GROSCHNER

2013

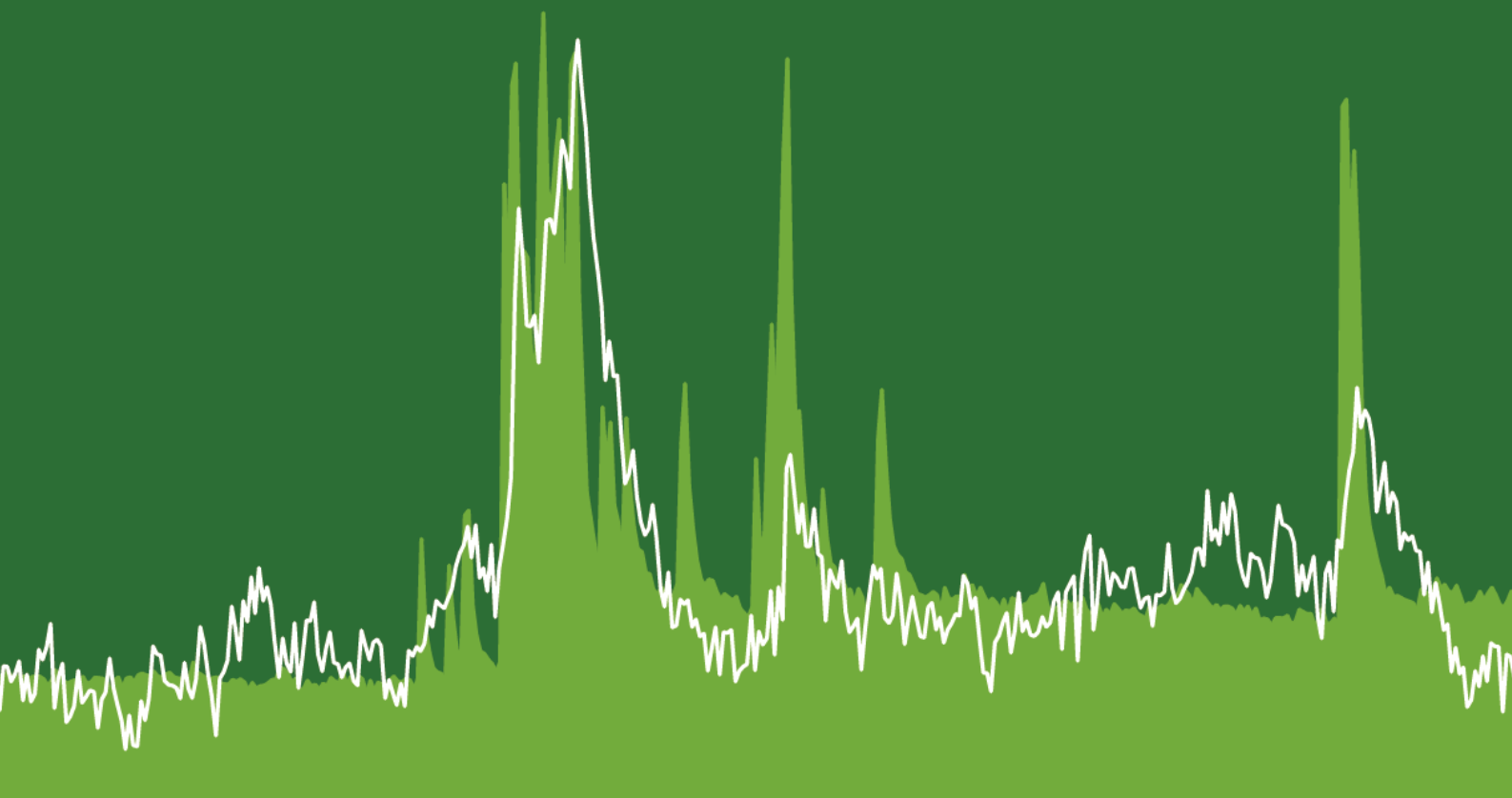

Diplomarbeit

METABOLISM-SECRETION COUPLING AND MITOCHONDRIAL CALCIUM ACTIVITIES IN PANCREATIC BETA-CELLS

eingereicht von

Lukas Groschner

Geb.Dat.: 16.11.1988

zur Erlangung des akademischen Grades

Doktor der gesamten Heilkunde (Dr. med. univ.)

an der

Medizinischen Universität Graz

ausgeführt am

Institut für Molekularbiologie und Biochemie

unter Anleitung von

Univ.-Prof. Dr. Wolfgang F. Graier

Assoz. Prof. Dr. Roland Malli

Graz, 2013

STATUTORY DECLARATION

I hereby declare that I have authored this thesis independently, that I have not used other than the declared sources/resources, and that I have explicitly marked all material which has been quoted either literally or by content from the used sources.

Graz, 31.05.2013 Lukas Groschner

EIDESSTATTLICHE ERKLÄRUNG

Ich erkläre an Eides statt, dass ich die vorliegende Arbeit selbstständig und ohne fremde Hilfe verfasst, andere als die angegebenen Quellen nicht verwendet, und die den benutzten Quellen wörtlich oder inhaltlich entnommenen Stellen als solche kenntlich gemacht habe.

Graz, 31.05.2013 Lukas Groschner

ACKNOWLEDGEMENTS

I would like to express my gratitude to all those people who have contributed to this work in various different aspects and who have inspired me throughout my studies. Especially I would like to thank

…Wolfgang Graier, who is probably the most enthusiastic supervisor a young scientist could wish for and who taught me how important it is to love what you do. Thank you for your trust, inspiration and the freedom you gave me. …Roland Malli, who was a seemingly endless fountain of clever and unconventional ideas throughout my studies.

…Rizwan, whom it was a great pleasure to work and share a project with, who had the patience to answer all my questions at any time of day or night, and with whom I hope to have plenty fruitful collaborations in not too distant future. …Patrik Rorsman for inviting me to Oxford and letting me thrive on his unprecedented expertise in islet cell electrophysiology. …Josephine Forbes and Melinda Coughlan for introducing me to the field of mitochondrial research. …Vi for being both the best teacher and friend on the southern hemisphere. …René for being the knight in shining armor he actually is, although he might not be aware of it. …Elisa for introducing me to confocal Ca^{2+} imaging. …Quan and Liang for teaching me how to isolate pancreatic islets. …Sonja for spreading serenity throughout the lab. …Claire, Markus, Jadoon, Neel, András, Warisara, Therese, Corina, Sasha, Sandra, Felix, Christiane, Nicole, Anna, Flo, Simone, Jan and Lissi for their help and hard work.

…my Mother and my Father for inspiring discussions, constructive criticism and their continuous unwavering support.

…Eva, whom I share everything with. Thank you for your confidence, your immeasurable help and endless patience.

This work was supported by a Student Research Fellowship of the Medical University of Graz.

ABSTRACT

Pancreatic β-cells are the only cells capable of lowering blood glucose by secreting insulin. The β-cell continuously adjusts its secretory activity to substrate availability in order to keep blood glucose levels within the physiological range – a process referred to as metabolism-secretion coupling. Glucose is readily taken up by the β-cell and broken down into intermediates that fuel oxidative metabolism inside the mitochondria to generate ATP. The resulting increase in the ATP/ADP ratio causes closure of plasma membrane K_{ATP}-channels, thereby depolarizing the cell and triggering the opening of voltage-gated Ca^{2+} channels. Consequential oscillations of cytosolic Ca^{2+} not only mediate the exocytosis of insulin granules, but are also relayed to other subcellular compartments including the mitochondria, where Ca^{2+} might act to accelerate mitochondrial metabolism in response to nutrient stimulation. The aim of this study was to investigate the role of two proteins involved in the uptake of Ca^{2+} by the mitochondria, mitochondrial Ca^{2+} uptake 1 (MICU1) and mitochondrial Ca^{2+} uniporter (MCU), in metabolism-secretion coupling of the pancreatic β-cell.

Employing an RNAi-mediated gene silencing strategy, I could selectively suppress the expression of MICU1 and MCU in INS-1 832/13 clonal pancreatic β-cells. Silencing of MICU1 and MCU significantly reduced mitochondrial Ca^{2+} signals after stimulation with glucose. Cells deficient of MICU1 or MCU also failed to sufficiently increase O_2 consumption rates and cytosolic ATP levels in response to high glucose. Glucose-stimulated insulin secretion was reduced by 57.7 and 41.8 % in cells treated with siRNA targeted against MICU1 or MCU, respectively.

The presented data illustrate the fundamental role of MICU1 and MCU in the feed-forward mechanism that guarantees sustained insulin secretion and thereby identify the mitochondrial Ca^{2+} uptake machinery as a promising therapeutic target for type 2 diabetes mellitus.

ZUSAMMENFASSUNG

Die Funktion der β-Zellen des Pancreas besteht darin, den Blutzuckerspiegel durch die Sekretion von Insulin zu senken. Zu diesem Zweck muss die β-Zelle ihre sekretorische Aktivität fortwährend an schwankende Glucosekonzentrationen anpassen – ein Prozess, der als Stoffwechsel–Sekretionskopplung bezeichnet wird. Glucose wird dabei von der β-Zelle aufgenommen und treibt über die Bildung von Pyruvat den oxidativen Soffwechsel der Mitochondrien an. Der dadurch bedingte Anstieg des ATP/ADP-Verhältnisses führt zum Schließen von K_{ATP}-Kanälen in der Plasmamembran und so zur Depolarisation der Zelle. Über die Öffnung von spannungsabhängigen Ca^{2+}-Kanälen kommt es daraufhin zu zytosolischen Ca^{2+}-Oszillationen, die einerseits die Exozytose insulingefüllter Vesikel auslösen, andererseits aber auch prompt in andere Zellkompartimente, einschließlich der Mitochondrien, fortgeleitet werden. Über die Aktivierung Ca^{2+}-abhängiger Enzyme der mitochondrialen Matrix kommt es so zu einer zusätzlichen Verstärkung der ATP-Produktion und damit auch der Insulinsekretion.

Die vorliegende Arbeit hat zum Ziel, den Beitrag von MICU1 und MCU, zweier Proteine, die in die mitochondriale Ca^{2+}-Aufnahme involviert sind, zur Stoffwechsel-Sekretionskopplung der β-Zelle zu untersuchen. Unter Anwendung von RNAi-vermitteltem Gen-silencing konnte ich die Expression von MICU1 und MCU in INS-1 832/13 Zellen selektiv hemmen. Gen-Knockdown von MICU1, wie auch von MCU unterdrückte die Glucose-induzierten mitochondrialen Ca^{2+}-Signale und verminderte zugleich den Anstieg des zellulären O_2-Verbrauches, als auch der ATP-Synthese nach Stimulation mit Glucose. Die Behandlung mit siRNA gegen MICU1 oder MCU führte außerdem zum Abfall der Glucose-induzierten Insulinsekretion um 57,7 bzw. 41,8 %.

Diese Ergebnisse verdeutlichen die grundlegende Rolle von MICU1 und MCU im Ca^{2+}-vermittelten positiven Feedback-Mechanismus, der eine adäquate Insulinsekretion ermöglicht und definieren dadurch mögliche neue Therapieziele für eine Behandlung des Diabetes mellitus Typ 2.

TABLE OF CONTENTS

LIST OF PUBLICATIONS

This thesis comprises a compendium of the following peer-reviewed articles:

1. M.R. Alam, **L.N. Groschner**, W. Parichatikanond, L. Kuo, A.I. Bondarenko, R. Rost, M. Waldeck- Weiermair, R. Malli, W.F. Graier. Mitochondrial Ca^{2+} uptake 1 (MICU1) and mitochondrial Ca^{2+} uniporter (MCU) contribute to metabolism-secretion coupling in clonal pancreatic β-cells. *J Biol Chem*. 2012 Oct 5;287(41):34445-54.

2. **L.N. Groschner**, M.R. Alam, W.F. Graier. Metabolism-secretion coupling and mitochondrial calcium activities in clonal pancreatic beta-cells. (*Manuscript*).

3. Q. Zhang, R. Ramracheya, C. Lahmann, A. Tarasov, M. Bengtsson, O. Braha, M. Braun, M. Brereton, S. Collins, J. Galvanovskis, A. Gonzales, **L.N. Groschner**, N.J.G. Rorsman, A. Salehi, M.E. Travers, J.N. Walker, A.L. Gloyn, F. Gribble, P.R.V. Johnson, F. Reimann, F.M. Ashcroft, P. Rorsman. Paradoxical K_{ATP} channel closure causes glucose-induced inhibition of glucagon secretion and impaired counter-regulatory response in type-2 diabetes. (*Manuscript*).

Other contributions:

4. J.M. Forbes, B.-X. Ke, T.-V. Nguyen, D.C. Henstridge, S.A. Penfold, A. Laskowski, K.C. Sourris, **L.N. Groschner**, M.E. Cooper, D.R. Thorburn, M.T. Coughlan. Deficiency in mitochondrial complex I activity due to Ndufs6 gene trap insertion induces renal disease. *Antioxid Redox Signal*. 2013 (in press).

5. M. Waldeck-Weiermair, A.T. Deak, **L.N. Groschner**, M.R. Alam, C. Jean-Quartier, R. Malli, W.F. Graier. Molecularly distinct routes of mitochondrial Ca^{2+} uptake are activated depending on the activity of the sarco/endoplasmic reticulum Ca^{2+} ATPase (SERCA). *J Biol Chem*. 2013 May 24;288(21):15367-79.

6. A.T. Deak, **L.N. Groschner**, M.R. Alam, E. Seles, A.I. Bondarenko, W.F. Graier, R. Malli. The endocannabinoid N-arachidonoyl glycine (NAGly) inhibits store-operated Ca^{2+} entry by abrogating STIM1/Orai1 interaction. *J Cell Sci*. 2013 Feb 15;126(Pt 4): 879-88.

7. M.J. Khan, M.R. Alam, M. Waldeck-Weiermair, F. Karsten, **L. Groschner**, M. Riederer, S. Hallström, P. Rockenfeller, V. Konya, A. Heinemen, F. Madeo, W.F. Graier, R. Malli. Inhibition of autophagy rescues palmitic acid induced necroptosis of endothelial cells. *J Biol Chem*. 2012 Jun 15;287(25):21110-20.

8. **L.N. Groschner**, M. Waldeck-Weiermair, R. Malli, W.F. Graier. Endothelial mitochondria – less respiration, more integration. *Pflügers Arch*. 2012 Jul; 464(1):63-76.

LIST OF ABBREVIATIONS

$[Ca^{2+}]_{cyto}$	cytosolic free Ca^{2+} concentrations
$[Ca^{2+}]_{mito}$	mitochondrial free Ca^{2+} concentration
ADP	adenosine-5'-diphosphate
ANOVA	analysis of variance
ATP	adenosine-5'-triphosphate
AU	arbitrary units
BSA	bovine serum albumin
CCD	charge-coupled device
cDNA	complementary DNA
CGP-37157	7-Chloro-5-(2-chlorophenyl)-1,5-dihydro-4,1-benzothiazepin-2(3*H*)-one
cLuc	cytosolic luciferase
CoA	coenzyme A
C_T	cycle threshold
DMEM	Dulbecco's Modified Eagle Medium
DNA	deoxyribonucleic acid
dNTP	deoxyribonucleotide triphosphate
EB	experimental buffer
EDTA	ethylenediaminetetraacetic acid
EGTA	ethylene glycol tetraacetic acid
ELISA	enzyme-linked immunosorbent assay
ER	endoplasmic reticulum
ETC	electron transport chain
FCCP	carbonyl cyanide-4-(trifluoromethoxy)phenylhydrazone
Fis1	mitochondrial fission 1 protein
Fluo-4 AM	Fluo-4-acetoxymethyl ester

FRET	Förster resonance energy transfer
Fura-2 AM	Fura-2-acetoxymethyl ester
GAPDH	glyceraldehyde 3-phosphate dehydrogenase
GLUT1/2	glucose transporter 1/2
GSIS	glucose-stimulated insulin secretion
GTP	guanosine-5'-triphosphate
HBSS	Hank's buffered salt solution
HEPES	4-(2-hydroxyethyl)-1-piperazineethanesulfonic acid
IMM	inner mitochondrial membrane
K_{ATP} channel	ATP-sensitive K^+ channel
LDCV	large dense core vesicle
LDH	lactate dehydrogenase
LETM1	leucine zipper EF-hand-containing protein 1
LSM	laser scanning microscope
MCT1	monocarboxylate transporter-1
MCU	mitochondrial Ca^{2+} uniporter
MCUR1	mitochondrial Ca^{2+} uniporter regulator 1
mGDH	mitochondrial glycerophosphate dehydrogenase
MICU1	mitochodrial Ca^{2+} uptake 1
MODY	maturity onset diabetes of the young
mRNA	messenger RNA
mtDNA	mitochondrial DNA
mtGTP	mitochondrial GTP
NAD^+	nicotinamide adenine dinucleotide
NCLX	mitochondrial 3 Na^+/Ca^{2+} (Li^+) exchanger
NMRI	Naval Medical Research Institute
OCR	oxygen consumption rate

OXPHOS	oxidative phosphorylation
PB	pre-incubation buffer
PBS	phosphate-buffered saline
PC	pyruvate carboxylase
PCR	polymerase chain reaction
PDH	pyruvate dehydrogenase
RIPA	radioimmunoprecipitation assay
RNA	ribonucleic acid
RNAi	RNA interference
RNase	ribonuclease
rpm	revolutions per minute
RPMI-1640	Roswell Park Memorial Institute-1640
RyR1	ryanodine receptor 1
S100A1	S100 calcium-binding protein A1
SEM	standard error of the mean
siRNA	small interfering RNA
TAE	tris-aceteate-EDTA
TCA cycle	tricarboxylic acid cycle
UCP	uncoupling protein
VDCC	voltage-dependent Ca^{2+} channel
$\Delta\Psi_{mito}$	inner mitochondrial membrane potential

LIST OF FIGURES

1 INTRODUCTION

The pancreatic β-cell is a particularly exciting type of cell, not only because its membrane harbors voltage-gated ion channels, which by definition make it an electrically excitable cell, but especially because of its unique way of adjusting secretory activity to substrate availability. There are not many cell types that are capable of accomplishing similar tasks and most certainly no other type of cell can secrete insulin, the one and only blood glucose-lowering hormone (1). Depletion or dysfunction of β-cells is unavoidably linked to the development of diabetes mellitus, a disease currently affecting over 6.4 % of adults worldwide (2) and causing one death every seven seconds (3). Along with the prevalence of this disease, diabetes-associated healthcare costs are also increasing at an enormous speed, accounting already for 2 to 7 % of national healthcare expanses in Western Europe (4), hence, placing a growing burden on both individual patients and national economies.

In order to provide better insight into the pathophysiology of diabetes mellitus, a detailed understanding of the process of insulin secretion is of utmost importance and has thus turned the pancreatic β-cell into an attractive target for both basic and clinical research. In the 1960s it was found that metabolic substrates and intermediates other than glucose had a similar effect on insulin secretion and that inhibition of intracellular metabolism is sufficient to prevent insulin secretion even in the presence of glucose (5). These observations have led to the idea that glucose elicits insulin release through metabolism of the hexose within the β-cell rather than through interaction with a specific receptor, thus ruling out the concept of a surface bound "glucoreceptor".

Since then, the exceptional way of adjusting insulin secretion to the availability of metabolic substrates, a process also referred to as "metabolism-secretion coupling", has attracted a lot of attention. In essence, this is achieved by different K_{ATP} channel-dependent and -independent mechanisms (6, 7). The uptake of glucose by the β-cell through glucose transporter 1 in humans and 2 in rodents and its oxidative metabolism yields a rise in the cytosolic ATP/ADP ratio. This, in turn, decreases the K_{ATP} channel's open probability (8,

9), thus reducing the β-cell's membrane potential and causing the opening of voltage-gated Ca^{2+} channels. Triggered by the influx of Ca^{2+}, insulin-filled vesicles subsequently release their cargo and thereby lower blood glucose levels (**Figure 8**)(10).

The dependence of glucose-stimulated insulin secretion (GSIS) on cytosolic Ca^{2+} activity has been known for more than half a century. Over the past 30 years, however, more and more evidence has accumulated, supporting the notion that not only cytosolic Ca^{2+} activity but also its propagation to other cellular organelles are essential for the β-cell to adequately fulfill its function. Especially the mitochondria as central hub connecting oxidative metabolism to insulin secretion have proven to hinge on Ca^{2+} in order to maintain and adjust their metabolic function (11). This study focuses on the role of mitochondrial Ca^{2+} handling in metabolism-secretion coupling of clonal pancreatic β-cells.

1.1 The importance of mitochondria to β-cell function

Electron micrographs have shown that mitochondria are frequently found within close proximity to secretory granules of β-cells (**Figure 1c**) (12). This observation already points to an integral role of this organelle in the process of insulin secretion. However, the study of mitochondrial physiology in pancreatic β-cells is more or less limited to methods that allow the assessment of mitochondrial function in intact cells, since the quantity of β-cell mitochondria that can be isolated from primary islets is comparatively small and potentially contaminated with mitochondria from other islet cells. Yet, recent technical advancements in the field of fluorescent sensors have opened up new possibilities of studying mitochondrial function in one given cell on multiple levels in parallel (13, 14). Such sensors can be used in primary cells, but are particularly applicable in β-cell lines in order to investigate basic concepts in β-cell physiology. Several widely used clonal cell lines have proven to be valuable in overcoming the shortage and limitations of primary β-cells (15, 16) and have helped to study mitochondrial function in this very special type of cell.

The functional integrity of mitochondria is fundamental to β-cell physiology, which is highlighted by the finding that depletion of mitochondrial DNA (mtDNA) causes severe impairment of GSIS in β-cell lines such as MIN6 (17, 18) and INS-1 (19). Certain types of

diabetes are linked to mutations affecting mitochondrial function. Mutations in hepatic nuclear factor 1-α, for example, lead to uncoupling of mitochondrial oxidative phosphorylation (OXPHOS) in INS-1 cells and are associated with type 3 of maturity onset diabetes of the young (MODY3) (20). β-cell-specific knockout of the mitochondrial transcription factor A also causes impaired insulin secretion and loss of β-cell mass resulting in a form of mitochondrial diabetes in mice (21). Mutations in mtDNA have been proposed to account for 0.5 to 1 % of all cases of diabetes in humans (22). Taking into consideration that the majority of all mitochondrial proteins are coded for by nuclear DNA, it can be assumed that the actual prevalence of mitochondrial diabetes is exceeding these estimates. Increasing evidence implicates not only mutations in mtDNA, but also environmental factors such as a surfeit of metabolic substrates and a concomitant increase in reactive oxygen species in the pathogenesis of mitochondrial dysfunction, thus, uncovering the mitochondrion as one of the major culprits in the development of impaired glucose tolerance and diabetes mellitus (23).

The general importance of mitochondrial metabolism to the process of GSIS is reflected by the fact that inhibition of the mitochondrial adenine nucleotide translocase, responsible for transporting ATP out of and ADP into the mitochondrial matrix, completely abolishes glucose-induced electrical activity of β-cells, indicating that glycolysis-derived ATP is not sufficient to maintain proper function (24). Overexpression of the adenine nucleotide translocase in INS-1 cells, however, does not potentiate O_2 consumption rates (OCRs), Ca^{2+} signals or insulin secretion in response to glucose (unpublished observations), prompting the idea that the transport of ADP/ATP across mitochondrial membranes is not a rate-limiting factor. Inorganic phosphate, which is required by complex V of the electron transport chain to synthesize ATP, is transported into the mitochondria via a phosphate carrier. Silencing of this carrier decreases ATP production and insulin secretion in response to glucose (25). Pharmacological dissipation of the mitochondrial inner membrane potential ($\Delta\Psi_{mito}$) using protonophores, effectively inhibits β-cell secretory activity despite an increase in cytosolic Ca^{2+} (26), emphasizing the relevance of the spatiotemporal coordination of metabolic and ionic signals. Similar to protonophores, also

overexpression of mitochondrial uncoupling protein 1 (UCP1), which reduces the coupling of OXPHOS, results in decreased ATP production, increased K_{ATP} channel activity, hyperpolarized plasma membrane potential and drastically impaired GSIS in a mouse β-cell line (27). It is noteworthy, however, that a potentiation of insulin secretion, such as that evoked by glucagon-like peptide-1, is not necessarily associated with an increase in OXPHOS (28) prompting the idea that mitochondrial energy metabolism is essential for insulin secretin, but stimulation of GSIS does not always involve changes in energy metabolism.

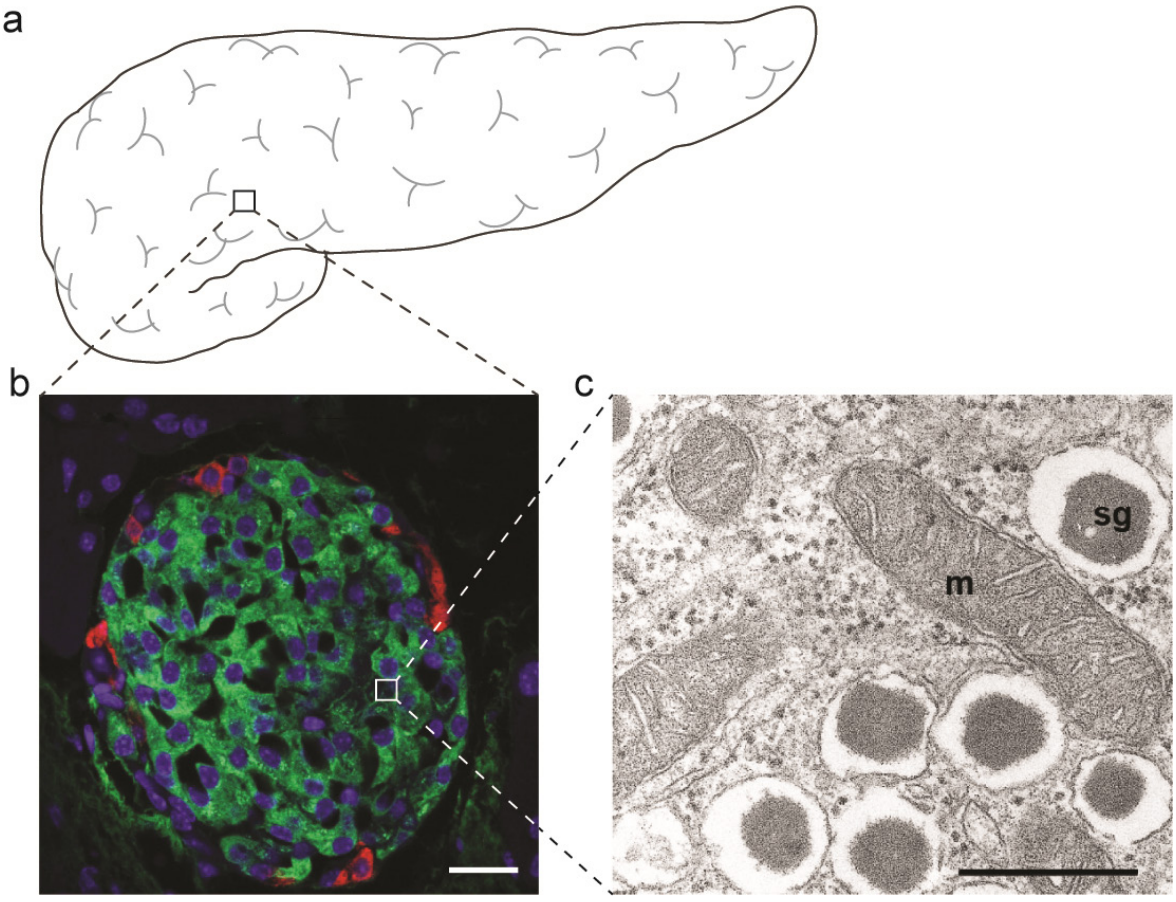

Figure 1. Pancreatic β-cell mitochondria. a, The pancreas contains both exocrine and endocrine cells, the latter of which are distributed throughout the organ forming cell clusters referred to as the pancreatic islets. **b,** Fluorescent micrograph of a mouse islet of Langerhans immunostained for the two primary blood glucose-regulating hormones: insulin (green) and glucagon (red). Nuclei were counterstained with 4',6-diamidino-2-phenylindole (blue). The scale bar represents 20 μm. The image was kindly provided by M. Solimena. **c,** Electron micrograph showing part of a pancreatic β-cell. Mitochondria (m) are juxtaposed to insulin-filled secretory granules (sg). The scale bar represents 500 nm. Reprinted from (29).

1.2 Mitochondrial integrity and β-cell function

Mitochondria constitute an interconnected filamentous network of moving organelles continuously changing their shape through fission and fusion events (30). Dynamics and ultrastructure of this organelle are inseparably linked to its bioenergetic function (31). Fis1, an integral component of the mitochondrial fission machinery, seems to be of particular importance to metabolism-secretion coupling. INS-1E cells overexpressing Fis1 exhibit fragmented mitochondria and fail to hyperpolarize $\Delta\Psi_{mito}$ when challenged with high glucose. Interestingly, also mitochondrial Ca^{2+} uptake and GSIS were significantly reduced under these conditions (32). In the same study, overexpression of a dominant negative mutant of mitofusin 1 led to similar morphological changes but did not impede GSIS, indicating that changes in mitochondrial structure are not necessarily accompanied by changes on the functional level. These discrepancies might be explained by additional unknown functions of Fis1 or by differential effects on mitochondrial motility. Knockdown of Fis1 resulted in decreased O_2 consumption and - just like its overexpression - in reduced GSIS (33).

Investigating the function of proteins involved in mitochondrial Ca^{2+} sequestration, we have described the fragmentation of mitochondrial networks in β-cells overexpressing MICU1 (34), pointing out the bidirectional relationship between Ca^{2+} homeostasis, morphology and motility of mitochondria. The Ca^{2+} sensitivity of mitochondrial dynamics is mediated by an EF-hand containing Miro GTPase, which causes mitochondria to halt at sites of high cytosolic Ca^{2+} concentrations ($[Ca^{2+}]_{cyto}$) (35). It is tempting to speculate that this phenomenon contributes to the fact that β-cell mitochondria regularly localize at subplasmalemmal Ca^{2+} hotspots near the readily releasable pool of secretory granules (**Figure 1**) (12) where they might have important functions in controlling local dynamics of Ca^{2+}, ATP and other coupling factors (36).

1.3 Oxidative metabolism of β-cells

The metabolism of the β-cell is quite distinctive as it is directly coupled to the primary cellular function, exceeding the mere task of supplying the cell with energy-rich molecules.

In addition, the β-cell has special preferences when it comes to metabolic substrates. So far a number of substances have been shown to stimulate insulin secretion, the most relevant of these being D-glucose. The branched-chain amino acid leucine and - to a lesser extent - free fatty acids are also amongst the nutrients that evoke insulin secretion. Various hormones and neurotransmitters potentiate insulin secretion via interaction with specific receptors. The main nutrient secretagogues, in contrast, undergo metabolism within the β-cell - more precisely, within its mitochondria - to create second messengers, which then influence β-cell electrical activity and thereby give rise to insulin exocytosis (37).

Metabolic intermediates that serve as source of energy during physical exercise or catabolic states, such as pyruvate, lactate or ketone bodies, need to be ignored by the β-cell in order to avoid hypoglycemic episodes (11). This apparent fuel selectivity requires the cell to express a very specific set of enzymes that make it possible to favor certain substrates, i.e. glucose, over others. In this regard the expression of specific genes has emerged to be just as important as the disallowance of others (38, 39). Loss of the β-cells' ability to discriminate between different substrates has been linked to phenotypes associated with inadequate insulin secretion. In contrast to primary islet cells (40), INS-1 insulinoma cell lines, for example, express significant amounts of the plasma membrane monocarboxylate transporter-1 (MCT1) and thus exhibit robust secretory response also after stimulation with pyruvate (41). A similar phenomenon can be observed in patients manifesting exercise-induced hyperinsulinism, where loss of the β-cell-specific silencing of MCT1 accounts for insulin secretion at times when it is least needed – in response to physical exercise (42). Using a mouse model overexpressing MCT1 in β-cells, it was recently demonstrated that the transport of pyruvate across the plasma membrane is sufficient to induce this form of hyperinsulinism (43).

Being the primary end-product of glycolysis, pyruvate represents a key metabolite in β-cells and not only its oxidation within the mitochondria but also its exchange with tricarboxylic acid (TCA) cycle intermediates have been shown to correlate with glucose responsiveness in different INS-1 cell lines (44). It can hence be assumed that the recently identified mitochondrial pyruvate carrier (45, 46) is essential for intact metabolism-secretion

coupling in β-cells, but its exact role in this context is still awaiting clarification. Once pyruvate has entered the mitochondrial matrix, it can be converted to acetyl-CoA by the pyruvate dehydrogenase (PDH), a protein complex that indirectly depends on free Ca^{2+} in its activity, or it can be carboxylated to form oxaloacetate via the pyruvate carboxylase (PC). Either way, pyruvate enters the TCA cycle and thereby fuels the mitochondrial electron transport chain. Lactate dehydrogenase (LDH) is an enzyme that prevents pyruvate from entering oxidative metabolism by converting it into lactate and regenerating NAD^+ needed during glycolysis. Correspondingly, INS-1 cell clones expressing high levels of LDH fail to accelerate O_2 consumption rates and insulin secretion in response to high glucose (47). Under normal conditions, NADH generated through glycolysis is efficiently shuttled into the mitochondria where it acts as another glycolysis-derived factor fueling mitochondrial metabolism (48).

Unlike most other cell lines, glucose responsive INS-1 cells have the remarkable ability to further boost their respiratory rate in response to increasing levels of glucose. Strictly speaking this phenomenon can be considered a reverse Crabtree effect: Under high-glucose conditions most clonal (tumor) cell lines tend to reduce OXPHOS to a minimum and solely rely on anaerobic glycolysis in order to meet their energy demands (49). To the β-cell, however, ATP is more than just an energy-rich molecule as its intracellular concentration is coupled to insulin secretion. In order to adjust granule exocytosis to glucose concentrations over a wide dynamic range, ATP synthesis is required to closely reflect glucose supply. If the β-cell would start generating only two molecules of ATP per molecule of glucose instead of the 30 to 32 that can be achieved through OXPHOS (50), the moment glucose levels exceed a certain threshold, it could clearly not keep up with the increasing insulin demand. For this reason β-cells need to increase their OCRs even further under high-glucose conditions. Extracellular glucose concentration relates to the rate of glucose oxidation in a sigmoidal curve with the steepest slope between concentrations of 5.5 and 8 mM of glucose (5) thereby corresponding very well to OCRs, (**Figure 5a**) and GSIS.

There are certain sub-clones of the INS-1 insulinoma cell line, which differ considerably in terms of their secretory response to high glucose. A recent study has linked these differences in metabolism-secretion coupling to the expression levels of genes related to OXPHOS. Any functional defects causing a Warburg-like shift from mitochondrial to anaerobic glycolytic metabolism were found to result in decreased glucose responsiveness of clonal β-cells and also correlate with the severity of a preexisting diabetic phenotype in humans (47). Taken together, these findings highlight the importance of mitochondrial oxidative metabolism in GSIS.

1.4 Mitochondrial coupling factors

Mitochondria represent the central hub of cellular bioenergetics and are also an organelle with crucial roles in cell signaling (30). In the pancreatic β-cell these two functions overlap in many ways as the mitochondria are the main source not only of ATP but also of a multitude of other signaling molecules, which have been shown to regulate insulin secretion (29).

The amino acid glutamate, for example, is formed from α-ketoglutarate in β-cell mitochondria during glucose stimulation and has been proposed to act as a mitochondrial signal driving the ATP-independent amplifying phase of insulin secretion (51). Although this concept has been challenged by others using alternative means to increase cytosolic glutamate concentrations (52), measurements of membrane capacitance have revealed a direct effect of glutamate on insulin granule exocytosis (53). Accordingly, disrupting either the generation of glutamate by knocking out glutamate dehydrogenase (54) or its transport out of the mitochondrial matrix by silencing the mitochondrial glutamate carrier (55) impedes GSIS.

Mitochondrial GTP (mtGTP), another potent signaling molecule, forms within the mitochondrion as a byproduct of the TCA cycle in the reaction of succinyl-CoA to succinate and is not exported to the cytosol. Two different isoforms of succinyl-CoA synthetase couple this reaction to the generation of either one molecule of ATP or GTP. Silencing of the ATP-producing isoform resulted in a pronounced increase in GSIS while

knockdown of the GTP-producing form had a negative effect on GSIS (56). Surprisingly, this shift from ATP to mtGTP synthesis was accompanied by a drop in $\Delta\Psi_{mito}$, an increase in O_2 consumption and a potentiation of cytosolic Ca^{2+} activity despite a reduction in ATP. Given that mtGTP-depleted cells showed an increase in overall mitochondrial Ca^{2+} concentration ($[Ca^{2+}]_{mito}$) after stimulation with glucose, the authors argue that mtGTP might act to promote the extrusion of Ca^{2+} from the mitochondria, hence, diverting the proton motive force from ATP production to the electrogenic Na^+/Ca^{2+} exchange. A more recent study implicates mtGTP in controlling mitochondrial production of phosphoenolpyruvate, another factor amplifying GSIS (57). Future work will be needed to elucidate the mechanisms behind mitochondrial GTP-signaling.

Mitochondrial matrix pH, a parameter closely reflecting metabolic activity, naturally correlates very well with nutrient activation in INS-1E cells. Yet, matrix pH seems to affect metabolism-secretion coupling independent of its influence on the electrochemical gradient across the inner mitochondrial membrane (IMM) as proposed by a study using the unspecific K^+/H^+ ionophore nigericin to induce matrix acidification (58). Further studies will be needed to identify the molecular mechanisms underlying this phenomenon.

Most of these coupling factors are likely to contribute to the feed-forward mechanism elicited by mitochondrial Ca^{2+} activity, which contributes mainly to the second phase of insulin secretion (59).

1.5 Ca^{2+} handling in β-cells

Glucose stimulates insulin secretion exclusively in the presence of Ca^{2+}, which is illustrated by the fact that hypocalcaemic conditions can impair GSIS (60). Intracellular free Ca^{2+} takes central stage in the process of GSIS by directly triggering exocytosis of insulin-filled large dense core vesicles (LDCVs). Several proteins encoded by the synaptotagmin gene family have been implicated in the Ca^{2+}-dependency of vesicle membrane fusion (61) while others like syntaxin and synaptosomal protein of 25 kDa seem to be required for tight coupling between voltage-dependent Ca^{2+} channels and LDCVs (62). Close physical interaction between local sites of Ca^{2+} entry and the exocytotic apparatus is necessary to

guarantee efficient utilization of cytosolic free Ca^{2+}, which is limited even during electrical activity of the β-cell. This might be attributable to a comparatively low plasma membrane Ca^{2+} channel density (63). Under resting conditions $[Ca^{2+}]_{cyto}$ is kept around 90 nM and even during stimulation overall cytosolic Ca^{2+} hardly exceeds concentrations of 400 nM (64). Intracellular application of 10 mM of the Ca^{2+}-chelating agent EDTA does not prevent granule exocytosis (65), indicating that the β-cell has apparently developed a very efficient system of cellular Ca^{2+} handling to secure both insulin secretion and the transfer of Ca^{2+} signals from subplasmalemmal microdomains to cellular compartments such as the mitochondria (66).

1.6 Mitochondrial Ca^{2+} and energy metabolism

A rise of intracellular Ca^{2+} is generally associated with cell activation and, thus, with a concomitant increase of cellular energy expenditure. Under these conditions, a vast amount of ATP is utilized within the cell for specific functions such as contraction, ion transport, protein synthesis, motility or exocytosis (67). In order to meet the increased energy demands, most cells are able to accelerate OXPHOS in dependence of cellular Ca^{2+} levels and so is the β-cell. Facing rapid, pulsatile changes of $[Ca^{2+}]_{cyto}$ during stimulation with glucose (**Figure 2**), the β-cell can significantly boost both its O_2 consumption and ATP production rates compared to basal conditions (cf. **Figure 5** and **6**) (59). In the absence of extracellular Ca^{2+}, increases in response to glucose are comparatively modest (**Figure 6a**) (59), but still detectable, suggesting that the initial stimulation of mitochondrial metabolism by glucose does not necessarily require extracellular Ca^{2+}. The following acceleration of OXPHOS, in contrast, strictly depends on the presence of extracellular Ca^{2+}.

Yet, cytosolic Ca^{2+} has conflicting effects on mitochondrial metabolism. On the one hand, being a cation, its uptake into the mitochondrial matrix per se causes depolarization of $\Delta\Psi_{mito}$, thereby reducing the driving force for ATP synthesis. In β-cells such transient depolarization occurs shortly after glucose-evoked cytosolic Ca^{2+} peaks and can be prevented by removal of extracellular Ca^{2+} (68). On the other hand, free Ca^{2+} acts as an

activating signal for mitochondrial dehydrogenases, thus providing the electron transport chain with an increasing amount of reducing equivalents (69). Based on mathematical modeling of β-cell Ca^{2+} activity, Magnus and Keizer proposed in 1998 that the former would outweigh the latter effect. According to their β-cell model, the glucose-induced uptake of Ca^{2+} by mitochondria would cause a drop in $\Delta\Psi_{mito}$ in the range of 0.8 mV with slow temporal kinetics, but sufficient to suppress ATP synthesis to an extent that causes opening of K_{ATP} channels, thus implicating mitochondrial Ca^{2+} uptake in the termination of electrical bursting in the β-cell (70, 71). This theoretical model, however, is not in line with experimental data from both cell lines and primary β-cells gathered since that time (14, 34, 59).

Despite its pivotal role as a second messenger, Ca^{2+} can also be harmful to the cell when its concentration exceeds a threshold over a certain period of time. Apart from the deleterious effects of a persistent elevation of $[Ca^{2+}]_{mito}$ on mitochondrial permeability transition and the initiation of cell death (72), prolonged intracellular Ca^{2+} signals observed under maximal stimulation with agonists accelerate mitochondrial metabolism only transiently, whereas oscillations of frequencies >0.5/min, as typically seen in stimulated β-cells (cf. **Figure 2**), provoke a sustained activation of Ca^{2+}-dependent mitochondrial dehydrogenases (73).

1.7 Ca^{2+}-dependent proteins within the mitochondria

A possible influence of Ca^{2+} ions on mitochondrial metabolism was first suggested in the late 1950s and was thereafter confirmed by Denton and McCormack who demonstrated that the activity of three key mitochondrial dehydrogenases is sensitive to Ca^{2+} (74). PDH, one of the rate-limiting enzyme complexes of oxidative metabolism, is activated via dephosphorylation by PDH phosphatase, an enzyme highly dependent on the concentration of free Ca^{2+} (75). Isocitrate-dehydrogenase and α-ketoglutarate-dehydrogenase, two TCA cycle enzymes in contrast are regulated by direct binding of Ca^{2+} (76, 77). In addition to these, a plethora of other mitochondrial metabolic enzymes have been reported to contain Ca^{2+}-binding domains and, thus, represent likely contributors to

the integration of cellular Ca^{2+} signals. The EF-hand protein S100A1, for instance, has been shown to activate the ATP synthase itself via Ca^{2+}-dependent interaction with its F1 portion (78). The mitochondrial glycerophosphate dehydrogenase (mGDH) is another Ca^{2+}-regulated enzyme. As part of the glycerol phosphate shuttle, mGDH is localized to the outer part of the IMM allowing glycolysis-derived NADH to enter oxidative metabolism within the mitochondria (79). It was speculated that an islet specific deficiency in mGDH activity might even contribute to the pathogenesis of type 2 diabetes (80). The mechanisms behind the Ca^{2+}-dependent increase of OXPHOS are manifold and involve both direct and indirect actions of Ca^{2+} on mitochondrial proteins. This increase of OXPHOS can be observed even beyond the immediate actions of Ca^{2+} (81). After pre-stimulation with either high K^+ or a K_{ATP} channel blocker, MIN-6 cells exhibit an amplified response to glucose when compared to naïve cells (82).

Sound evidence for the activating role of mitochondrial Ca^{2+} in β-cells was provided by Wiederkehr and colleagues, who used a Ca^{2+}-buffering protein targeted to the mitochondrial matrix to modulate free matrix Ca^{2+} and found that buffering of $[Ca^{2+}]_{mito}$ resulted in reduced cellular respiration, ATP production and a decrease in the amplifying phase of insulin secretion (59).

1.8 Mitochondrial Ca^{2+} handling

Since the early 1960s it is known that respiring mitochondria are able to accumulate significant quantities of Ca^{2+} ions (83), but today we are only beginning to understand the molecular basis of this intricate phenomenon. After entering the cytosol, Ca^{2+} ions have to permeate both the outer and inner mitochondrial membrane before reaching the mitochondrial matrix. While the outer membrane constitutes less of a burden to ions and molecules smaller than 5 kDa, ion fluxes across the IMM are tightly regulated. So far a number of proteins, comprising ion channels, exchangers and regulatory proteins have been described to contribute to the shuttling of Ca^{2+} into and out of the mitochondrial matrix. Putative mitochondrial Ca^{2+} channels include the ryanodine receptor 1 (RyR1) (84), uncoupling proteins 2 and 3 (UCP2/3) (85) and the mitochondrial Ca^{2+} uniporter

(MCU). MCU is a two transmembrane domain protein of the IMM representing the putative pore-forming subunit of what turns out to be a multi protein MCU-complex (86, 87). Within this complex MCU associates with multiple regulatory proteins, the first of which MICU1 was discovered in 2010 by Mootha and colleagues screening a compendium of IMM proteins (88). MICU1 has one transmembrane domain and two EF-hand motifs on the matrix side that are crucial for its Ca^{2+}-sensing properties. More recent studies have suggested MICU1 as a negative regulator of the MCU, preventing mitochondrial Ca^{2+} overload under resting conditions (89). MICU2 and MICU3, two additional paralogs of MICU1, have also been identified and might contribute to the tissue specificity of mitochondrial Ca^{2+} handling (90). Mitochondrial Ca^{2+} uniporter regulator 1 (MCUR1) is another novel regulatory protein that has been reported to act in concert with MCU (91). UCP2/3 have been found particularly important in adjusting mitochondrial Ca^{2+} uptake to differences in the concentration (92) and the source (93) of cytosolic Ca^{2+}. In contrast to UCP2/3, which preferentially localize at contact sites between the mitochondria and the ER, the mitochondrial Ca^{2+}/H^{+} antiporter leucine zipper EF-hand-containing protein 1 (LETM1) (94) seems to be responsible for the transfer of Ca^{2+} entering the cell through channels in the plasma membrane of endothelial cells (95). Similar differential Ca^{2+} uptake mechanisms might have important functions in β-cells, where the extracellular milieu rather than intracellular stores represents the main source of Ca^{2+}.

Single channel patch-clamp recordings in mitoplasts isolated from HeLa cells have so far revealed the presence of at least three inwardly rectifying Ca^{2+} currents of different amplitudes (96, 97) pointing to the existence of multiple routes of mitochondrial Ca^{2+} uptake. To date, studies addressing the putative mitochondrial Ca^{2+} uptake pathways in β-cells are still to be carried out. Identification of the molecular machineries responsible for Ca^{2+} sequestration by β-cell mitochondria might not only provide better understanding of β-cell physiology but could also help uncover novel therapeutic targets for the treatment of type 2 diabetes.

1.9 Aims of the study

This study was designed to assess the function of MICU1 and MCU, two proteins involved in mitochondrial Ca^{2+} transport, in clonal pancreatic β-cells and their role in metabolism-secretion coupling.

The specific aims were:

1. To characterize mitochondrial Ca^{2+} activities in clonal pancreatic β-cells.
2. To explore the contribution of MICU1 and MCU to mitochondrial Ca^{2+} uptake in INS-1 832/13 cells.
3. To determine the effects posttranscriptional gene silencing of MICU1 and MCU on glucose-stimulated O_2 consumption, ATP production and insulin secretion.

2 MATERIALS AND METHODS

2.1 Chemicals and buffer solutions

All cell culture products were purchased from PAA Laboratories (Pasching, Austria) unless otherwise specified. Chemicals and reagents were obtained from Carl Roth (Karlsruhe, Germany) or Sigma-Aldrich (Vienna, Austria). All buffer solutions were prepared using ultrapure water from a Milli-Q® Integral Water Purification System (Merck Millipore, Germany). The composition of the buffers was as follows (in mM):

Tris-aceteate-EDTA (TAE) buffer: 40 Tris, 20 acetic acid and 1 EDTA.

Hank's buffered salt solution (HBSS): 114 NaCl, 4.7 KCl, 2.5 $CaCl_2$, 1.2 $MgCl_2$, 2 HEPES, 1.2 KH_2PO_4, 25 $NaHCO_3$ and variable concentrations of D-glucose as indicated, pH adjusted to 7.4 using NaOH.

Pre-incubation buffer (PB): 138 NaCl, 5 KCl, 2 $CaCl_2$, 1 $MgCl_2$, 1 HEPES, 2.6 $NaHCO_3$, 0.44 KH_2PO_4, 0.34 Na_2HPO_4, 10 D-glucose, 0.1 % vitamins, 0.2 % essential amino acids, and 1 % penicillin/streptomycin, pH adjusted to 7.4 with NaOH.

Experimental buffer (EB): 138 NaCl, 5 KCl, 2 $CaCl_2$, 1 $MgCl_2$, 10 HEPES and 10 D-glucose, pH adjusted to 7.4 with NaOH. In buffer solutions containing high concentrations of KCl, isoosmolarity was maintained by reducing the concentration of NaCl accordingly.

Phosphate-buffered saline (PBS): 137 NaCl, 2.7 KCl, 10 Na_2HPO4, 1.8 KH_2PO_4, pH adjusted to 7.4 with NaOH.

Radioimmunoprecipitation assay (RIPA) buffer: 50 Tris, 150 NaCl, 0.1 % sodium dodecyl sulfate, 0.5 % sodium deoxycholate, 1 % Triton X 100, 5 % protease inhibitor cocktail.

2.2 Cell culture

Experiments were carried out using the rat insulinoma cell line INS-1 832/13 stably expressing the human proinsulin gene. These cells exhibit a robust secretory response to glucose which can be attributed to both K_{ATP}-dependent and –independent pathways (16). The culture medium used was RPMI-1640 supplemented with 11.1 mM D-glucose, 10 %

fetal calf serum, 2 mM L-glutamine, 1 mM sodium pyruvate, 10 mM HEPES, 100 U/ml penicillin, 100 µg/ml streptomycin and 50 µM β-mercaptoethanol. Cells were cultured in 6-well tissue culture plates at 37 °C gassed with 5 % CO_2 in a humidified atmosphere. For experiments only cells between population doublings 47 and 70 were used.

2.3 Islet isolation

For gene expression analysis, pancreatic islets were isolated from C57/BL6J mice. Mice in between 9 and 12 weeks of age were killed by cervical dislocation and the peritoneal cavity was opened carefully avoiding contamination. Under the stereomicroscope, the common bile duct was identified and ligated as close to the major duodenal papilla as possible using either surgical silk or a small clamp, making sure that the suture is placed distal to the junction with the pancreatic duct (ampulla of Vater). The common bile duct was subsequently cannulated from the proximal side using a 30G needle and a forceps and the pancreas was perfused retrogradely with ~3 ml of HBSS containing 1 mg/ml of collagenase type V (Sigma Aldrich, Austria) until fully distended. In the case of leakage or incomplete distention, the pancreas was microinjected with collagenase solution. The distended pancreas was then removed as a whole, transferred into sterile 15 ml tubes and incubated in a water bath at 37 °C for 12 min after adding another 2 ml of collagenase solution. Digestion was stopped by adding 10 ml of ice cold HBSS containing 0.2 % of BSA. After washing the digested tissue three times with cold HBBS, islets were handpicked under the stereomicroscope, transferred to RPMI-1640 medium supplemented with 5 mM D-glucose and kept in the incubator at 37 °C for up to 24 hours before starting experiments. For measurements of $[Ca^{2+}]_{cyto}$ an analog procedure was applied to NMRI mice.

2.4 Transfection

Gene knockdown in INS-1 832/13 cells was achieved by transient transfection with a combination of two different siRNAs targeting either rat MICU1 or rat MCU. Transfection with scrambled siRNA was used as a negative control. Sequences of the siRNAs were 5'GUAAUGGAGUAUGAGAAUA and 5'CGAACCUGGUGAAACUGAA for rat MICU1,

5'GCCAGAGACAGACAAUACU and 5'AAAGTCTCGTTTCGACCTA for rat MCU and 5'AGGTAGTGTAATCGCCTTG as a negative control, not targeting any known rat gene. All siRNA sequences were designed by M.R. Alam (98). Cells were cultured in 6-well plates until reaching a confluency of 50-60 % before performing transfection using TransFast™ Transfection Reagent (Promega, USA), a lipofection-based method, according to the manufacturer's recommendations. A transfection mixture containing 200 pmoles/ml of respective siRNAs and/or 3 µg/ml of plasmid DNA as well as 8 µl/ml of TransFast™ Transfection Reagent was prepared in Dulbecco's Modified Eagle Medium (DMEM, Sigma, Austria) free of serum and antibiotics. After vortexing, the mixture was incubated for 15 min at room temperature. The growth medium was removed from 6-well plates and 500 µl/well of transfection mixture were added. Cells were incubated at 37 °C and 5 % CO_2 for 1 hour before replenishing each well with 500 µl of serum and antibiotics-free DMEM. After an incubation period of 18-20 hours, the cells were changed to complete growth medium. All experiments were performed 48-60 hours after transfection.

2.5 mRNA quantitation

2.5.1 RNA isolation

Total cellular RNA was isolated 48 hours after transfection using peqGOLD Total RNA Kit (PEQLAB, Germany) according to the manufacturer's recommendations. Culture medium was removed completely and INS-1 832/13 cells were lysed by adding 200 µl of RNA Lysis Buffer T per well of a 6-well plate, making sure that the surface area is fully submerged to guarantee complete lysis of all cells. The lysate was transferred onto a DNA Removing Column placed in a 1.5 ml reaction tube and centrifuged for 1 min at 12000 g (at room temperature). The flow through was then mixed with 200 µl of ice cold 70 % ethanol (in nuclease free H_2O) and transferred onto a PerfectBind RNA Column placed in a 2.0 ml collection tube. After 1 min of centrifugation at 10 000 g, the collection tube together with the flow through was discarded. The column was reinserted into a fresh collection tube and 500 µl of RNA Wash Buffer I were added before starting a 15 s centrifugation at 10 000 g. The flow through was discarded and 600 µl of RNA Wash Buffer II (complemented with

ethanol) were added to the column followed by another 15 s of centrifugation at 10 000 g. This second washing step was repeated once. In order to remove any traces of ethanol, the column was centrifuged for another 2 min at 10 000 g. The PerfectBind RNA Column was then transferred to a sterile 1.5 ml reaction tube and total RNA was eluted by adding 20 µl of nuclease-free H_2O followed by 1 min of centrifugation at 5 000 g. RNA concentration was determined using an UviLine 9400 spectrophotometer (SCHOTT Instruments, Germany). All RNA samples were stored at -70 °C until use.

2.5.2 Reverse transcription

Conversion of RNA into cDNA was achieved using the High Capacity cDNA Reverse Transcription Kit (Applied Biosystems, USA) on a Primus 25 advanced thermocycler (PEQLAB, Germany). The master mix was composed as follows (per 20 µl final reaction volume): 2.0 µl 10X RT Buffer + 2.0 µl 10X Random Primers + 0.8 µl dNTP Mix (100 mM) + 1.0 µl RNasin® Plus RNase inhibitor (Promega, USA) + 1.0 µl nuclease-free H_2O + 1.0 µl MultiScribe™ Reverse Transcriptase (50 U/µl). As template for cDNA synthesis, total cellular RNA was diluted with nuclease-free H_2O to a final concentration of 2 µg/10 µl. 10 µl of diluted RNA were added to 10 µl of master mix to create a 1X reaction mix. The thermocycler was programed to run a 4-step protocol: 25 °C for 10 min, 37 °C for 120 min, 85 °C for 5 min followed by infinite storage at 4 °C.

2.5.3 PCR

In order to verify expression of the respective genes of interest, PCR was performed employing the ready-to-use GoTaq® Green Master Mix (Promega, USA). For a 20 µl-reaction volume, 10 µl of 2X GoTaq® Green Master Mix, 7 µl of nuclease-free H_2O, 1 µl of upstream primer (10 µM), 1 µl of downstream primer (10 µM) and 1 µl of cDNA template were mixed. Primer sequences were 5'CTGGTGCTGAGTATGTCGTGGA and 5'AGTTGGTGGTGCAGGATGCATT for rat GAPDH (product size: 197 bp), 5'ACTAAGCGGAGACTGATGTTG and 5'GTCCTTGCTCTTCCCCTTATC for rat MICU1 (product size: 149 bp), 5'AGATGGTGTTCGAGTTGCTG and

5'AGGGTCTCTGCGTTTTCATG for rat MCU (product size: 138 bp), 5'TTGACTTGAATGGAGACGGAG and 5'AACATAAGCCAGACTTGAGGG for mouse MICU1 (product size: 138 bp), and 5'TCGACCTAGAGAAATACAATCAGC and 5'CACGGTCATCTCGGATCATTC for mouse MCU (product size: 137 bp). A Primus 25 advanced thermocycler (PEQLAB, Germany) was deployed to run the following program: 1 cycle of initial denaturation (95 ˚C for 5 min), 40 cycles of denaturation (95 ˚C for 1 min), annealing (60 ˚C for 1 min) and elongation (72 ˚C for 1 min), 1 cycle of final extension (72 ˚C for 10 min) and infinite storage at 4 °C.

2.5.4 Gel electrophoresis

PCR products were visualized by agarose gel electrophoresis. A 1.5 % agarose solution was prepared in TAE buffer using a microwave. 10000X GelRed® Nucleic Acid Gel Stain (Biotium, USA) was added accordingly to create a final concentration of 1X GelRed®. The agarose solution was poured into a casting tray (including a comb) and let solidify. The gel was placed in an electrophoresis chamber filled with TAE buffer. PCR samples and DNA ladder (GeneRuler™ 100 bp, Thermo Fisher Scientific, Austria) were loaded on the gel and run at ~3 V/cm. Bands were visualized using a GenoSmart gel documentation system (VWR International).

2.5.5 Real time PCR

For relative quantitation of mRNA copies, quantitative real-time PCR was performed using LightCycler® 480 Real-Time PCR System (Roche, Switzerland) and QuantiFast® SYBR Green PCR Kit (Qiagen, Germany). Primer sequences used were the same as listed above and primer efficiencies were determined by analyzing different concentrations of pooled cDNA (1:10, 1:100 and 1:1000). Rat GAPDH was used as a housekeeping gene to normalize for differences in cDNA concentrations between samples. All samples were run in triplicate. Composition of 10 µl of reaction volume: 5 µl of 2X QuantiFast® SYBR Green PCR Master Mix, 1 µl of upstream primer (10 µM), 1 µl of downstream primer (10 µM), 2 µl of nuclease-free H_2O and 1 µl of cDNA (1:50). Reaction conditions were chosen

according to a standard LightCycler® protocol with an initial heat activation at 95 °C for 5 min followed by 40 cycles of 10 s at 95 °C (denaturation) and 30 s at 60 °C (annealing and extension). The cycle threshold (C_T) values were analyzed using the Relative Expression Software Tool (Qiagen, Germany).

2.6 Ca^{2+} measurements

2.6.1 $[Ca^{2+}]_{cyto}$ measurements in intact islets

Confocal Ca^{2+} imaging was accomplished as previously described (99). Intact, medium-sized islets from NMRI mice were loaded with 2 µM of the Ca^{2+} indicator Fluo-4 AM (Invitrogen) in RPMI-1640 medium containing 5 mM of D-glucose for 3 hours at room temperature. After loading, islets were transferred to fresh medium without Fluo-4 AM for another 30 min before starting experiments. Laser scanning confocal microscopy was performed using a LSM 510 meta system on an upright microscope (Axioskop 2 FS, Zeiss, Germany) equipped with a micromanipulator. In the perifusion chamber, islets were hold in place using a wide-bore holding pipette and perifused throughout the experiment with HBSS containing D-glucose and KCl as indicated. All experiments were conducted at a bath temperature of 35-37 °C. Fluo-4 was excited with an Argon laser at 488 nm, and emission light was captured using a 500-550 nm band-pass filter and a photomultiplier. Fluorescence intensities were normalized to peak values after addition of 30 mM KCl.

2.6.2 $[Ca^{2+}]_{mito}$ measurements

INS-1 832/13 cells were cultured on 30 mm glass slides and co-transfected with respective siRNAs and a genetically encoded, FRET-based Ca^{2+} sensor targeted to the mitochondrial matrix (4mtD3cpv). Measurements were conducted 48-72 hours after transfection on two different microscopy systems, which accounts for the different kinetics of $[Ca^{2+}]_{mito}$ signals in **Figure 4**. Traces displayed in **Figure 4a** were recorded using an Eclipse TE300 inverted microscope (Nikon, Japan) with a polychromator illumination system (Opti Quip, USA) and a CCD camera (Roper Scientific, Germany). Traces in **Figure 4b** were captured on an Axiovert inverted microscope (Zeiss, Austria) equipped with a polychromator and a CCD

camera (both from Visitron Systems, Germany). 4mtD3cpv was excited at 440 nm and emission was captured at 480 and 535 nm through a 40 x oil-immersion objective (Zeiss and Nikon) using a beam splitter (Visitron Systems). Cells were perifused with EB containing different concentrations of D-glucose as indicated.

2.6.3 Simultaneous measurement of $[Ca^{2+}]_{cyto}$ and $[Ca^{2+}]_{mito}$

Changes in $[Ca^{2+}]_{cyto}$ and $[Ca^{2+}]_{mito}$ were recorded simultaneously and ratiometrically on single cell level using a red-shifted cameleon targeted to the mitochondrial matrix in combination with Fura-2 as previously published (13). INS-1 832/13 cells transiently expressing 4mtD1GO-Cam were loaded with 2 µM Fura-2 AM in PB for 30 min at room temperature. Before starting experiments, cells were washed 3 times with PB. During measurements, cells were perfused at room temperature with EB containing specified concentrations of D-glucose. Fluorescent images were captured on a digital fluorescence microscope (Till iMIC, Till Photonics, Germany) using a 40 x oil-immersion objective (alpha Plan-Fluor, Zeiss, Germany) with a time interval of 1.5 s to minimize photobleaching. 4mtD1GO-Cam and Fura-2 were excited alternatingly at 340, 380 (Fura-2) and 477 nm (4mtD1GO-Cam) using a Polychrome V monochromator (Till Photonics, Germany), an excitation filter and a dichroic filter (both Chroma Technology Corp, USA). Emission was detected at 510 nm (Fura-2 and green-channel of 4mtD1GO-Cam) and 560 nm (yellow/FRET-channel of 4mtD1GO-Cam) using an emission filter (Chroma Technology Corp, USA), an additional dichroic filter (Till Photonics, Germany) and a CCD camera (Stingray F145, Allied Vision Technologies, Germany). Original recordings were corrected for photobleaching based on a one-phase exponential decay.

2.7 Measurement of cellular O_2 consumption

INS-1 832/13 cells were plated in XF96 polystyrene cell culture microplates (Seahorse Bioscience, USA) at a density of 50 000 cells per well and transfected with respective siRNAs as depicted above. On the day of the assay, cells were pre-incubated for 1 hour at 37 °C in glucose-free unbuffered XF assay medium (Seahorse Bioscience, USA). Oxygen

consumption rates (OCR) were measured with a time interval of 6 min using an XF96 extracellular flux analyzer (Seahorse Bioscience, USA). FCCP (carbonyl cyanide-4-trifluoromethoxyphenylhydrazone) was injected to determine maximal respiration at a final working concentration of 1 μM. Values were normalized to basal respiration.

2.8 $[ATP]_{cyto}$ measurements

$[ATP]_{cyto}$ was assessed by detecting bioluminescence in cells expressing cytosolic firefly luciferase (cLuc), an enzyme catalyzing a light emitting reaction in the presence of ATP and its substrate luciferin. INS-1 832/13 cells were seeded in white-walled 96-well microplates with a clear flat bottom (PerkinElmer Inc., USA) at a density of 70 000 cells/well and co-transfected with respective siRNAs and a plasmid encoding cLuc (kindly provided by Rosario Rizzuto) (36). 48 hours after transfection, the cells were pre-incubated for 1 hour in HBSS containing 0.2 % BSA and 3 mM D-glucose. The buffer was then replaced with HBSS containing 3 mM D-glucose and 1 mM beetle luciferin (Promega, USA). In order to maximize signal-to-noise ratio, the bottom of the plate was covered with a sheet of white paper from beneath before counting emitted photons from the top on a VICTOR Mulitlabel Reader (PerkinElmer Inc., USA) at 37 °C.

2.9 Insulin secretion measurements

INS-1 832/13 cells were cultured in 6-well plates and transfected with respective siRNAs according to the protocol depicted in **2.4** at a confluency of 60-70 %. 48 hours after transfection (at a confluency of 90-100 %), cells were washed two times with warm HBSS and pre-incubated for 1 hour in 2 ml/well HBSS containing 0.2 % BSA and 3 mM D-glucose at 37 °C gassed with 5 % CO_2. Following pre-incubation, the cells were washed once more and the buffer was replaced by 2 ml HBSS supplemented with 3 mM D-glucose. In order to measure basal insulin secretion, a 1 ml-sample of the supernatant was collected on ice after 60 min of incubation. The remaining supernatant was removed and the respective well was replenished with 2 ml HBSS containing 16 mM D-glucose. After 1 hour of incubation, another sample was collected. The samples were centrifuged for 5 min at

1 800 g and 4 °C to remove any floating cells and 500 µl of the supernatants were collected for further analysis. Insulin concentrations in the supernatants were determined using an enzyme immunoassay (Mercodia Rat Insulin ELISA, Mercodia AB, Sweden) according to the manufacturer's protocol. Samples were analyzed at a 1:10 dilution in calibrator 0. Due to variations in absolute insulin secretion in dependence of the passage number of cells, all values were normalized to basal insulin secretion at 3 mM D-glucose.

2.10 Protein quantitation

Following a brief washing step in cold PBS, cell lysis was performed with RIPA buffer (200 µl/well) and samples were subsequently collected using rubber cell scrapers. Following 3 freeze-thaw cycles in liquid nitrogen, the lysate was centrifuged at 14 000 rpm and 4 °C for 20 min. The supernatant was collected and subjected to protein quantitation employing a bicinchoninic acid assay (Pierce® BCA Protein Assay, Thermo Fisher Scientific Inc., USA). Samples were diluted 1:10 and 10 µl of diluted samples and respective BSA-standards (ranging from 0-2 µg/µl) were pipetted into clear 96-well microplates. After addition of BCA working reagent (150 µl/well), the plate was incubated at 37 °C for ~30 min. Absorbance was measured at 560 nm on a VICTOR^3 V Mulitlabel Reader (PerkinElmer Inc., USA).

2.11 Statistics and data analysis

Data were analyzed using OriginPro version 8.5.0 (OriginLab Corp., USA) and GraphPad Prism version 5.00 (GraphPad Software, USA) for Windows. Student's t-test or one-way analysis of variance (ANOVA) with Dunnett's post test was performed where appropriate to determine statistical significances. Significance was defined as $p<0.05$. The data are expressed as means ± standard error of the mean (SEM) unless otherwise specified.

3 RESULTS

3.1 Glucose elicits cytosolic and mitochondrial Ca^{2+} signals in pancreatic β-cells.

In order to characterize cytosolic Ca^{2+} signals in different cell types of the pancreatic islet I used the Ca^{2+} indicator Fluo-4 to image $[Ca^{2+}]_{cyto}$ in freshly isolated islets from NMRI mice. Glucagon-secreting α- and insulin-secreting β-cells were distinguished based on their functional characteristics. In both cell types exocytosis is tightly coupled to an increase in $[Ca^{2+}]_{cyto}$. α-cells, which release glucagon at low glucose concentrations, show cytosolic Ca^{2+}–bursts with a period of ~5 min at ambient glucose of ≤6 mM (**Figure 2a**, black trace). β-cells, however, respond to a step increase in glucose concentration with abrupt initiation of $[Ca^{2+}]_{cyto}$–oscillations (**Figure 2a**, red trace). Interestingly, certain subpopulations of β-cells within one islet exhibit different threshold glucose concentrations. Only 11 out of 111 β-cells (from 9 different islets) responded to 6 mM glucose; however, all 111 β-cells responded to glucose concentrations ≥16 mM with continuous $[Ca^{2+}]_{cyto}$-oscillations at a frequency of 1-5 peaks/min. To assess in how far such glucose-induced oscillations in β-cell $[Ca^{2+}]_{cyto}$ are transferred to the mitochondrial matrix, I used the clonal INS-1 832/13 β-cell line, which, in contrast to primary cells, can be easily transfected with plasmids encoding mitochondrial Ca^{2+} sensors such as 4mtD1GO-Cam and thus allow simultaneous measurements of $[Ca^{2+}]_{cyto}$ and $[Ca^{2+}]_{mito}$ (13). This cell line shows sustained secretory response to glucose (16) and also cytosolic Ca^{2+} signals are comparable to those of primary β-cells with an oscillation frequency of 0.5-5 peaks/min at 16 mM glucose (**Figure 2b**). Co-imaging of 4mtD1GO-Cam with Fura-2 allowed to examine correlations of $[Ca^{2+}]_{mito}$ and $[Ca^{2+}]_{cyto}$ with highest temporal resolution. Glucose-induced cytosolic Ca^{2+} spikes were instantly transferred to the mitochondrial matrix with a time lag of only 3-6 s. Ca^{2+} extrusion from β-cell mitochondria, however, displayed significantly slower kinetics compared to respective cytosolic signals (**Figure 2b,** inset). Rapid, repetitive spiking of $[Ca^{2+}]_{cyto}$ led to desensitization of mitochondrial Ca^{2+} uptake expressed by the fact that not every single cytosolic Ca^{2+} peak was also detectable inside the mitochondria.

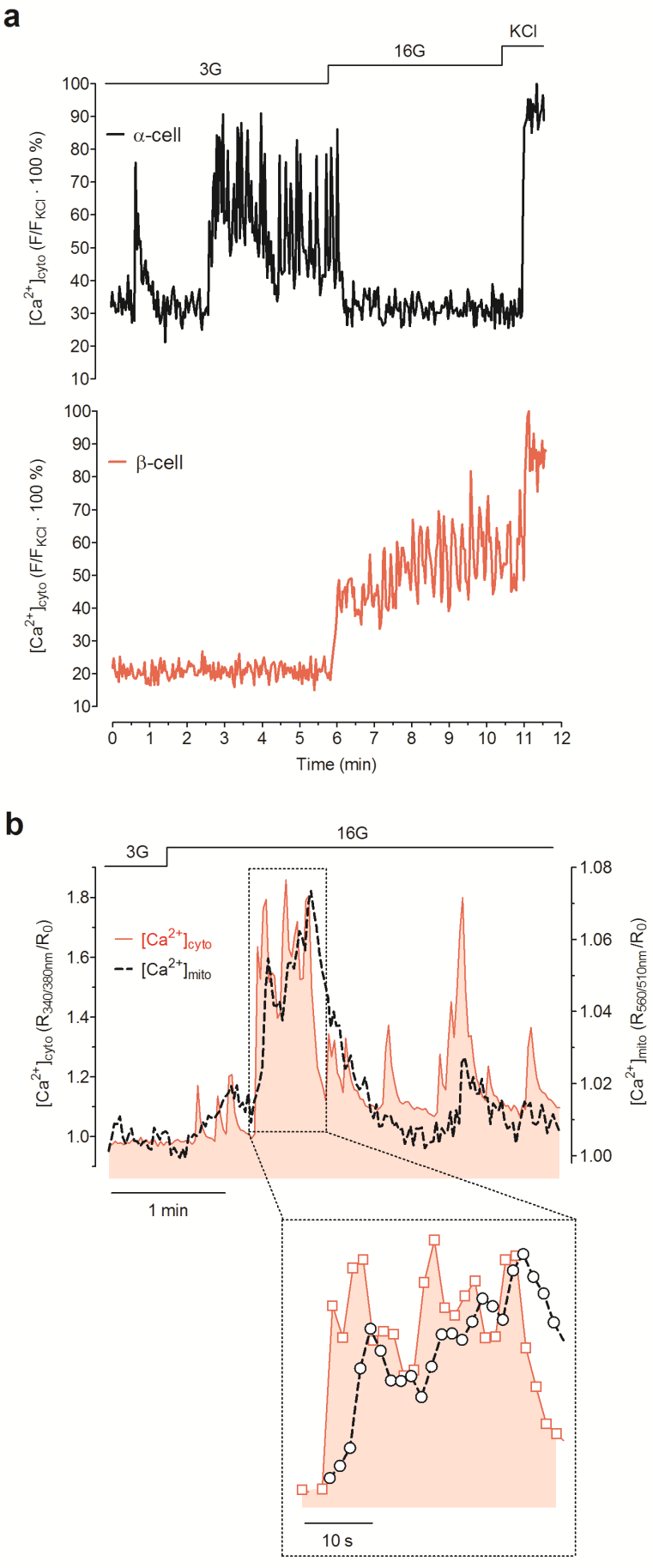

Figure 2. Glucose-induced Ca^{2+} signals in pancreatic islets and clonal β-cells. a, Cytosolic Ca^{2+} activity measured in a pancreatic α- (black trace, upper panel) and a juxtaposed β-cell (red trace, lower panel) in one intact pancreatic islet at 3 (3G) and 16 mM glucose (16G) and in response to 30 mM KCl (KCl). Traces are representative of recordings from 46 α- and 111 β-cells from 9 different islets. **b,** Correlation of glucose-induced cytosolic and mitochondrial Ca^{2+} signals in a clonal INS-1 832/13 β-cell. Similar to primary β-cells, stimulation with 16 mM glucose (16G) evoked oscillations of $[Ca^{2+}]_{cyto}$ (red trace). Cytosolic Ca^{2+} spikes were followed by respective peaks in mitochondrial Ca^{2+} (black dashed trace) with a delay of only 3-6 s. Ca^{2+} clearance from the mitochondrial matrix was slower as compared to the cytosolic compartment. The inset is showing a zoom-in image of the marked section.

3.2 Expression of MICU1 and MCU in pancreatic β-cells

After establishing and characterizing the stimulatory effect of glucose on $[Ca^{2+}]_{mito}$ in single β-cells, I sought to identify proteins responsible for this cell-specific mode of mitochondrial Ca^{2+} uptake. Two candidate proteins, MICU1 and MCU have recently been reported to be involved in the uptake of Ca^{2+} by mitochondria in different mammalian cell lines and tissues (86-88), but their role in β-cells remains enigmatic. Therefore, my aim was

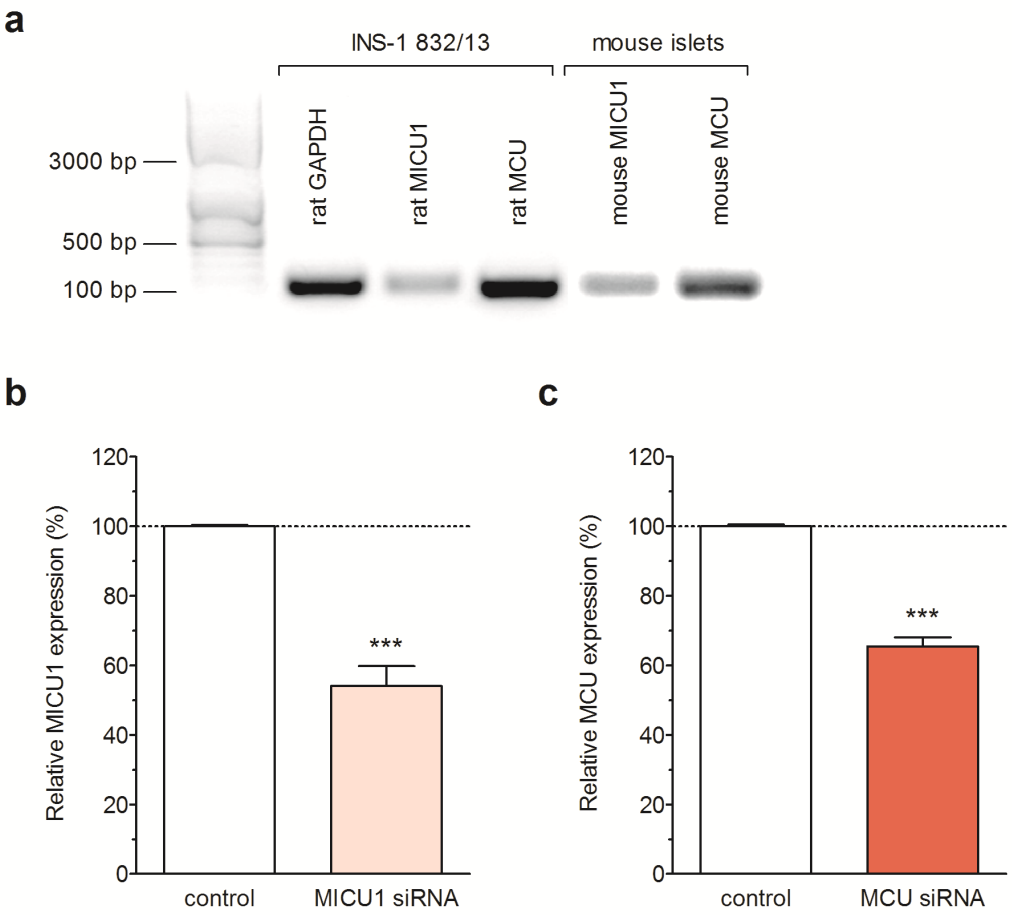

Figure 3. Expression of MICU1 and MCU in pancreatic β-cells can be reduced by RNAi. a, Agarose gel image confirming the expression of MICU1 and MCU in both isolated mouse islets and INS-1 832/13 cells. GAPDH was used as a positive control. **b,** Quantitative real-time PCR analysis of MICU1 expression in cells treated with scrambled control siRNA (control, n=6) or siRNAs targeted against MICU1 (MICU1 siRNA, n=7) 48 h after transfection. **c,** MCU expression 48 h after transfection with scrambled siRNA (control, n=3) or siRNAs targeting MCU (MCU siRNA, n=6). Bars represent means ± SEM; ***p<0.001.

to investigate the role of these two proteins in pancreatic β-cell function. MICU1 and MCU were detectable at the mRNA level both in primary mouse islets and in the clonal rat β-cell line INS-1 832/13 as confirmed by amplification of cDNA gene fragments using PCR primer pairs specific for the respective genes (for primer sequences see **2.5.3**). PCR products were visualized using agarose gel electrophoresis (**Figure 3a**). Confirmation at the protein level was not feasible due to a lack of reliable anti-rat MICU1 (CBARA1) or MCU (CCDC109A) antibodies. Yet, in order to explore the function of MICU1 and MCU, I employed an RNAi-based gene silencing strategy to create cells deficient of the respective proteins, which could subsequently be used in functional assays. To evaluate the efficiency of transient siRNA-mediated knockdown of MICU1 and MCU, quantitative real-time PCR was performed after isolating total RNA from cells transfected with a combination of two specific siRNAs targeting either MICU1 or MCU (for siRNA sequences see **2.4**). GAPDH was used as a housekeeping gene to normalize for differences in cDNA content. The number of mRNA copies was expressed relative to that of cells treated with scrambled control siRNA. Treatment with gene-specific siRNAs effectively reduced MICU1 mRNA levels to 54.0 ± 5.8 and MCU mRNA levels to 65.4 ± 2.6 % of control cells (**Figure 3b**).

3.3 Glucose-induced mitochondrial Ca^{2+} uptake is mediated by MICU1 and MCU

Having means to efficiently decrease the expression of MICU1 and MCU in clonal β-cells, I next sought to explore their contribution to the process of mitochondrial Ca^{2+} sequestration in this special cell type during stimulation with 16 mM glucose. For this purpose, INS-1 832/13 cells were co-transfected with the mitochondrial Ca^{2+} sensor 4mtD3cpv (mito-cameleon) and siRNAs targeting either MICU1 or MCU. 48 hours after transfection, glucose-starved cells were exposed to 16 mM glucose and changes in $[Ca^{2+}]_{mito}$ were recorded as described in **2.6.2**. 16 mM glucose triggered pronounced mitochondrial Ca^{2+} activities in control cells (**Figure 4a** and **c**, upper panels). In cells treated with siRNAs targeting either MICU1 or MCU, however, these signals were blunted, not to say abolished (**Figure 4a** and **c**, lower panels).

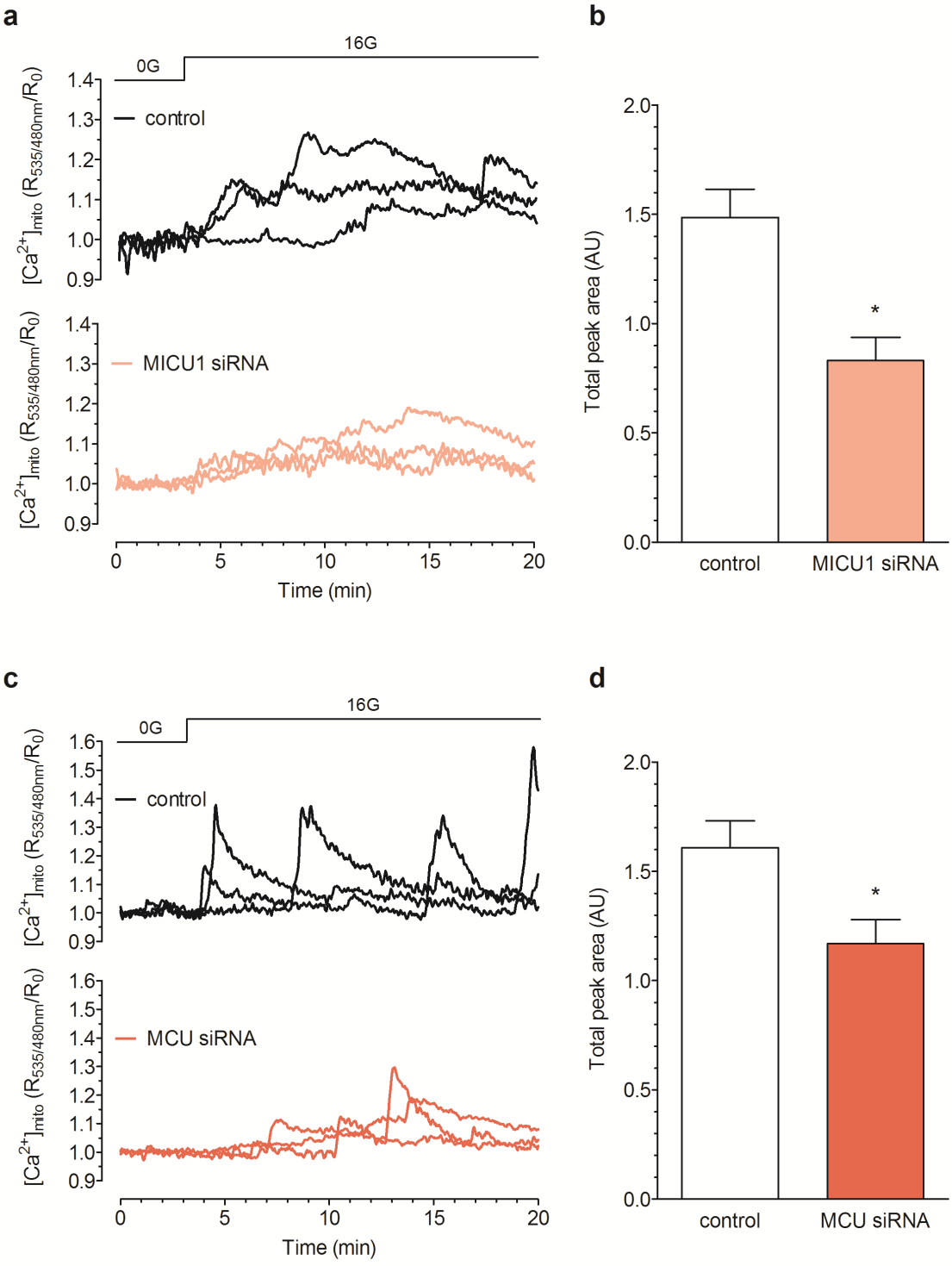

Figure 4. Knockdown of MICU1 and MCU decreases glucose-induced mitochondrial Ca^{2+} signals. Stimulation of INS-1 832/13 cells with 16 mM glucose (16G) elicited spiking of $[Ca^{2+}]_{mito}$. **a,** Representative $[Ca^{2+}]_{mito}$ recordings from cells treated with control (upper panel) and MICU1 siRNA (lower panel). **b,** Total peak area of curves from control (n=122 cells) and MICU1 knockdown cells (n=33 cells) after stimulation with 16G. *p=0.011. **c,** $[Ca^{2+}]_{mito}$ traces of control and MCU knockdown (MCU siRNA) cells exposed to high glucose. **d,** Total peak area of recordings from control (n=83 cells) and MCU-silenced cells (n=62 cells) after glucose exposure. Bars represent means ± SEM in arbitrary units (AU); *p=0.013.

Glucose-induced mitochondrial Ca^{2+} activities were heterogeneous/dyssynchronous in nature and amplitudes as well as frequencies of oscillations showed considerable variance over time and in between cells, making it difficult to analyze the recorded data quantitatively. To overcome this problem, traces were normalized to initial values and the total peak areas of individual curves were calculated. The total peak area after stimulation with glucose was 1.49 ± 0.12 AU in control and 0.83 ± 0.11 AU in MICU1-silenced cells. Silencing of MCU caused a drop in total peak area from 1.60 ± 0.13 to 1.17 ± 0.11 AU, indicating that both proteins promote glucose-triggered mitochondrial Ca^{2+} signals. Based on the observation that knockdown of either protein does not affect global $[Ca^{2+}]_{cyto}$ during glucose-stimulation (98), it can be reasoned that MICU1 and MCU, indeed regulate mitochondrial Ca^{2+} transport in clonal β-cells.

3.4 Knockdown of MICU1 affects mitochondrial oxidative metabolism

After confirming that MICU1 and MCU participate in mitochondrial Ca^{2+} uptake during glucose-stimulation (see **3.3**), I next wanted to explore to which extent MICU1- and MCU-mediated Ca^{2+} signals impact OXPHOS, the primary source of ATP in β-cells. Similar to native β-cells, INS-1 832/13 cells are able to boost their respiratory rates in response to glucose with a half maximal effective concentration of 6.2 mM glucose (**Figure 5a**). Maximal respiration as a measure of overall oxidative capacity, can be observed after dissipation of $\Delta\Psi_{mito}$ by addition of the protonophore carbonyl cyanide-4-(trifluoromethoxy)phenylhydrazone (FCCP) which showed a sigmoidal dose response curve with a half maximal effective concentration of 173.4 nM (**Figure 5b**). In subsequent experiments all cells were first stimulated with 16 mM glucose before determining maximal O_2 consumption by treatment with 1 µM FCCP (**Figure 5c**). Control cells increased their OCRs by a peak value of 22.9 ± 4.7 % in response to glucose, whereas cells deficient of MICU1 only showed a moderate increase of 7.4 ± 4.5 %; MCU-silenced cells responded to 16 mM glucose with a maximal increase in OCR of 16.1 ± 4.3 % (**Figure 5c** and **d**). 24 min after stimulation with glucose, O_2 consumption in cells deficient of MICU1 or MCU dropped to 98.6 and 108.1 % of basal, respectively. Control cells maintained respiratory

rates as high as 117.8 % of basal even after prolonged exposure to high glucose (**Figure 5c**), indicating that mitochondrial Ca^{2+} signals might be especially important for a sustained activation of TCA cycle dehydrogenases during the second (amplifying) phase of GSIS.

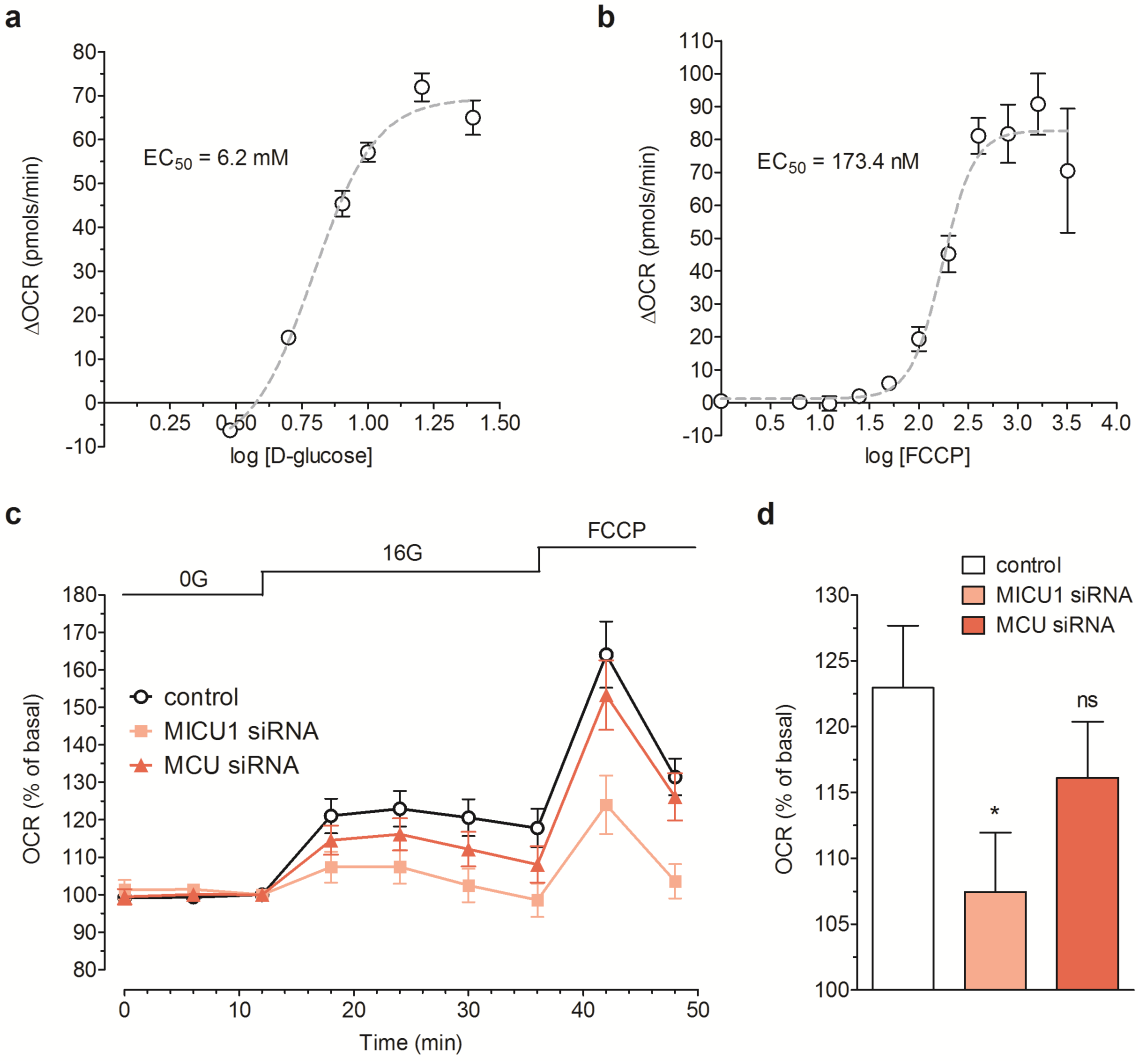

Figure 5. Silencing of MICU1 affects cellular O_2 consumption. a, INS-1 832/13 cells can increase their oxygen consumption rate (OCR) in response to glucose in a concentration-dependent manner with a half maximal effective concentration (EC_{50}) of 6.2 mM. **b,** Dose response curve for the uncoupling agent FCCP in INS-1 832/13 cells. EC_{50}=173.4 nM. **c,** OCRs of INS-1 832/13 cells treated with scrambled siRNA (control, n=20), siRNA targeting MICU1 (MICU1 siRNA, n=21) or MCU (MCU siRNA, n=21). Cells were pre-incubated in glucose-free medium (0G) and stimulated with 16 mM glucose (16G) and 1 µM FCCP at indicated time points. Data were normalized to basal values before stimulation with 16G and are shown as means ± SEM. **d,** Maximal OCRs after stimulation with 16G. *p=0.02, ns: not significant.

FCCP-induced maximal respiration was attenuated by knockdown of MICU1 but remained unchanged by knockdown of MCU. 1 µM FCCP provoked maximal OCRs of 164.1 ± 8.9 % in control cells, 124.0 ± 7.8 % in MICU1-deficient and 153.3 ± 9.3 % of basal in MCU-deficient cells (**Figure 5c**), suggesting that $[Ca^{2+}]_{mito}$ might also affect the overall oxidative capacity of β-cells.

3.5 MICU1 and MCU enhance glucose-triggered ATP synthesis

To test whether alterations in oxidative metabolism would also be detectable at the level of cellular ATP production, I measured changes in $[ATP]_{cyto}$ using INS-1 832/13 cells transiently expressing firefly-derived cLuc. This enzyme catalyzes a chemical reaction emitting photons in the presence of ATP, D-luciferin, Mg and O_2 and can thus be used to estimate subcellular ATP concentrations in a population of cells. In order to test the validity of this method in this particular setting, INS-1 832/13 cells were treated with 16 mM glucose, causing a steady increase in overall $[ATP]_{cyto}$ with peak values of 128.0 ± 3.2 % of basal (**Figure 6a**, black trace). The same experiment was performed in the presence of the ATP-synthase blocker oligomycin (2 µM) in combination with complex III inhibitor antimycin A (10 µM) as well as in the absence of extracellular Ca^{2+}. Ca^{2+}-free experimental conditions were achieved by addition of 400 nM of the Ca^{2+} chelator EGTA. Cells treated with ETC inhibitors, known to block ATP synthesis, showed a constant decline in overall $[ATP]_{cyto}$ (**Figure 6a**, light grey trace). Glucose-treatment in Ca^{2+}-free buffer caused an increase of only 14.8 ± 2.0 % (**Figure 6a**, grey trace). Taken together, these data indicate that this cLuc-based bioluminescent method provides efficient means to monitor changes in $[ATP]_{cyto}$ in response to glucose or ETC inhibitors and can also be used to detect alterations in $[ATP]_{cyto}$ secondary to alterations in Ca^{2+} signaling. Analog to experiments under Ca^{2+}-free conditions, cells deficient of MICU1 or MCU also failed to adequately increase $[ATP]_{cyto}$ in response to 16 mM glucose and showed a mean increase of only 16.2 ± 1.5 % and 20.3 ± 1.8 %, respectively (**Figure 6b**). These results are in line with both measurements of mitochondrial Ca^{2+} and O_2 consumption in β-cells (cf. **Figure 4** and

5) and point to an integral role of MICU1 and MCU in the decoding of cytosolic Ca^{2+} signals inside the mitochondria.

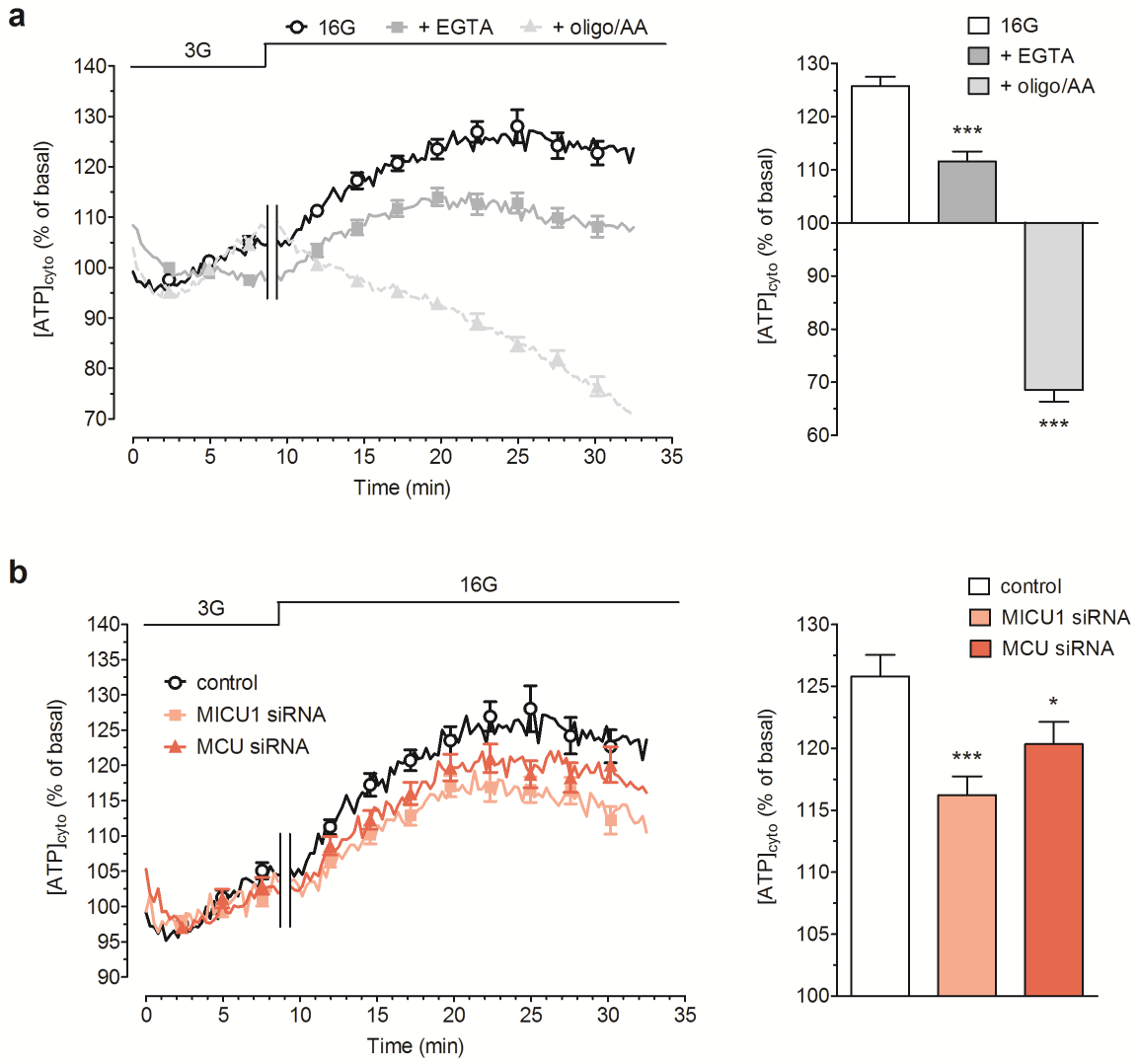

Figure 6. MICU1 and MCU contribute to the glucose-induced increase in $[ATP]_{cyto}$. a, INS-1 832/13 cells co-transfected with cLuc and control siRNA were treated with 16 mM glucose in the absence (16G, n=32) and presence of the Ca^{2+} chelator EGTA (+EGTA, n=24) or in the presence of 2 µM oligomycin and 10 µM antimycin A (+oligo/AA, n=30). Values were normalized to basal readings at 3 mM glucose (3G). Right panel: Mean $[ATP]_{cyto}$ after stimulation. ***p<0.0001 vs. 16G. **b,** $[ATP]_{cyto}$ in response to treatment with 16G measured in cells transfected with control siRNA (black, n=32), MICU1 siRNA (light red, n=32) and MCU siRNA (red, n=32). Right panel: Mean values after stimulation with 16G. ***p<0.0001, *p<0.05 vs. control.

3.6 MICU1 and MCU are required for sustained insulin secretion

Glucose represents the primary physiological trigger for insulin secretion. According to the consensus model of GSIS, ATP generated through mitochondrial OXPHOS prompts closure of plasma membrane K_{ATP} channels, depolarizing the cell and thus triggering electrical activity, which involves opening of voltage-dependent Ca^{2+} channels and causes insulin granule exocytosis (cf. **1.7** and **Figure 8**). After evaluating the effect of MICU1 and MCU knockdown at the levels of O_2 consumption (**3.4**) and ATP production (**3.5**), I attempted to explore the role of these two proteins in the principal function of a pancreatic β-cell, namely GSIS. Again, silencing of MICU1 and MCU in INS-1 832/13 cells was achieved by transient transfection with respective siRNAs. In order to exclude any RNAi-mediated unspecific effects on insulin biosynthesis, insulin content was measured in total cell lysates from all experimental groups. Transfection with respective siRNAs did not change cellular insulin content, which was 7.73 ± 0.17 in control, 7.62 ± 0.28 in MICU1-, and 7.29 ± 0.35 µg/mg protein in MCU-silenced cells (**Figure 7a**). GSIS, however, was drastically affected by knockdown of MICU1 and MCU. Stimulation with 16 mM glucose increased insulin secretion to 288.0 ± 17.3 % of basal levels in control cells. MICU1-deficient cells showed an increase to 179.5 ± 9.7 % and silencing of MCU reduced the effect of 16 mM glucose to 209.5 ± 19.6 % of basal (**Figure 7b**). In agreement with measurements of mitochondrial Ca^{2+}, O_2 consumption and cytosolic ATP, these data demonstrate the crucial involvement of MICU1 and MCU in the process of metabolism-secretion coupling in INS-1 832/13 cells.

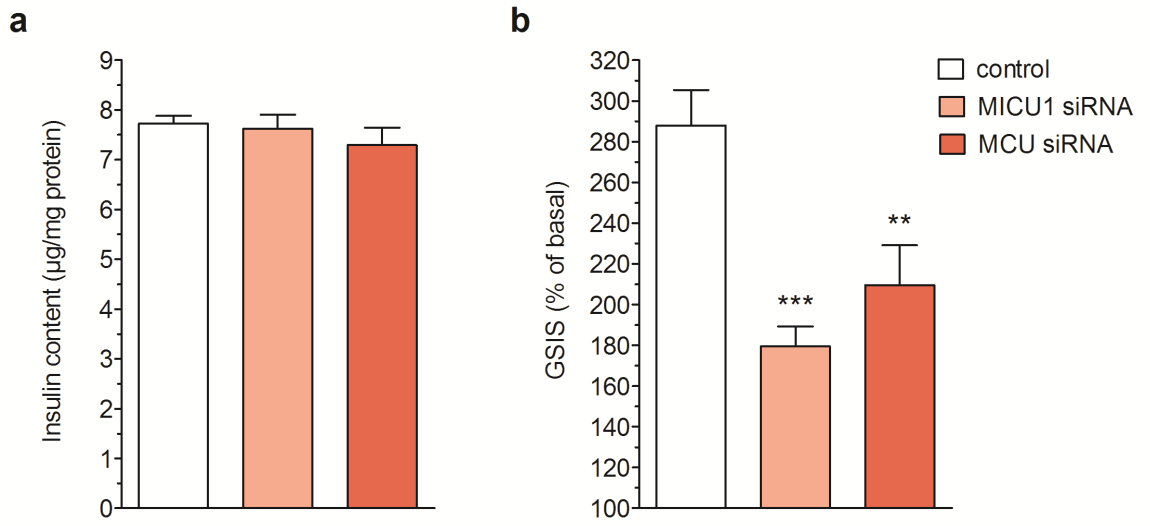

Figure 7. Knockdown of MICU1 and MCU impairs glucose-stimulated insulin secretion. a, Total cellular insulin content of cells treated with scrambled control siRNA (n=3) or siRNAs targeting MICU1 (n=3) or MCU (n=3). **b,** Insulin secretion was measured from the supernatants of INS-1 832/13 cells transfected with control siRNA (n=28), MICU1 siRNA (n=22) and MCU siRNA (n=12) after 1 hour of static incubation. GSIS at 16 mM glucose was normalized to basal values at 3 mM glucose. ***p<0.0001, **p<0.01 vs. control.

4 DISCUSSION

The data presented herein define a new mechanistic pathway for the stimulation of β-cell metabolism-secretion coupling by proteins involved in mitochondrial Ca^{2+} uptake. $[Ca^{2+}]_{mito}$ is of crucial importance to pancreatic β-cell function, which is to secrete insulin in response to elevated blood glucose. A step increase in extracellular glucose concentration causes an ATP-mediated increase in plasma membrane electrical resistance, depolarizing the cell and thereby triggering electrical activity. L-type Ca^{2+} channels, which are rapidly activated during the upstroke of action potentials, account for bulk cytosolic Ca^{2+} signals under these conditions (**Figure 2**), while Ca^{2+} influx via P/Q-type channels is required for exocytosis (63). A certain subpopulation of mitochondria are believed to be situated close to the inner mouth of L-type, possible also P/Q-type Ca^{2+} channels next to secretory granules (**Figure 1**) where they are confronted with oscillations of $[Ca^{2+}]_{cyto}$ at a high frequency. Therefore the β-cell's mitochondria regulate their Ca^{2+} uptake differently as compared to other, non-excitable cell types such as endothelial or HeLa cells (13) and are able to take up Ca^{2+} at incredibly high rates as reflected by the steep slope of mitochondrial Ca^{2+} increases (**Figure 2b,** black dashed trace) tightly following respective cytosolic spikes (**Figure 2b,** red trace). This instant transfer of cytosolic Ca^{2+} oscillations to the mitochondrial matrix has been proposed to activate metabolic enzymes and thereby amplify the production of mitochondrial coupling factors such as ATP (cf. **Figure 8**).

In this context the kinetics of mitochondrial Ca^{2+} signals are of special interest; yet, in many cases imaging techniques permit only limited inferences to be drawn about these. Using a recently developed genetically encoded, FRET-based mitochondrial Ca^{2+} sensor, it was possible to record mitochondrial and cytosolic Ca^{2+} signals in parallel on the single cell level. This approach provides means to study subcellular Ca^{2+} handling with unprecedented temporal and spatial resolution while maintaining an excellent signal to noise ratio (**Figure 2**) (13).

In contrast to Ca^{2+} influx, Ca^{2+} extrusion from β-cell mitochondria displays significantly slower kinetics not only compared to respective cytosolic peaks (**Figure 2b**), but also to other cell types (13), hence allowing for maximal amplification of Ca^{2+} signals needed to maintain metabolic activity. However, cytosolic Ca^{2+} peaks below a certain threshold are not detectable within the mitochondrial matrix (**Figure 2b**), which might be explainable by different Ca^{2+} affinities of channels themselves or of luminal Ca^{2+}-sensing subunits such as MICU1. This could also account for the time-dependent desensitization of mitochondrial Ca^{2+} sequestration observed during persistent stimulation (**Figure 2b**) (13). Effectively, the mitochondria seem to be able to modify both their Ca^{2+} uptake and their Ca^{2+} buffering capacity according to the metabolic needs of the cell.

Efflux of Ca^{2+} from the mitochondrial matrix is generally accomplished by the mitochondrial $3\,Na^+/Ca^{2+}$ (Li^+) exchanger (NCLX), driven by the inwardly directed electrochemical gradient for Na^+ (100) and can be inhibited using the benzothiazepine CGP-37157 (101). The idea of blocking the NCLX in order to amplify mitochondrial Ca^{2+} signals and thereby also metabolic rates has led to a series of experiments testing the effect of CGP-37157 on pancreatic β-cell function. Initial tests performed in INS-1 cells as well as rats found that treatment with this compound had a positive effect on both ATP production and GSIS in a dose- and glucose-dependent manner (102). Similarly, a more recent study showed that treatment with CGP-37157 is beneficial in restoring ATP levels and GSIS in an in vitro model of mitochondrial diabetes (MODY4) (103). Modulating NCLX activity might, in any case, represent efficient therapeutic means of preserving metabolic function under conditions of mitochondrial deficiency not only in β-cells (104). Based on these observations it can be hypothesized that not only Ca^{2+} release from, but also Ca^{2+} uptake by mitochondria might play a role in modulating β-cell function.

MICU1 and MCU are two proteins recently described to be implicated in mitochondrial Ca^{2+} uptake (86-88). In order to assess their function in clonal pancreatic β-cells and their role in metabolism-secretion coupling I employed an RNAi-based gene silencing strategy to suppress the expression of MICU1 and MCU in INS-1 832/13 cells (**Figure 3**). Silencing of MICU1 and MCU blunted mitochondrial Ca^{2+} signals in response to 16 mM glucose

(**Figure 4**) while leaving both frequency and amplitude of cytosolic Ca^{2+} oscillations unaffected (34, 98). A combined knockdown of MICU1 and MCU did not result in any additional decrease in mitochondrial Ca^{2+} uptake, suggesting that these two proteins are indeed part of the same Ca^{2+} uptake pathway (34, 98). Cells deficient of MICU1 also showed a clear reduction in O_2 consumption after glucose-stimulation as compared to control cells (**Figure 5**). This effect was less pronounced in MCU-deficient cells, probably reflecting variations in gene knockdown efficiency (**Figure 3**) rather than differences in gene function. The efficiency of posttranscriptional gene silencing is crucial when it comes to working with a population of cells and thus not being able to select transfected cells individually. The quantitative analysis of each experiment, however, is reminiscent of the reduction of gene expression achieved by treatment with siRNAs, which was slightly lower for MCU compared to that of MICU1 (**Figure 3**).

In accordance with OCR-measurements, an abrupt rise of extracellular glucose was followed by a progressive increase in $[ATP]_{cyto}$ (**Figure 6**), which was significantly attenuated in MICU1- and to a lesser extent also in MCU-deficient cells. The discrepancy between the effect on $[ATP]_{cyto}$ and GSIS despite a lack of effect on cytosolic Ca^{2+} (34, 98) might favor the idea of subplasmalemmal microdomains of high $[Ca^{2+}]_{cyto}$ undetectable by the methods employed in these studies. Expression of a Ca^{2+}-buffering protein targeted to the mitochondrial matrix also remained without effect on $[Ca^{2+}]_{cyto}$ (59). Again, this could be explained by the existence of localized Ca^{2+} hot spots or by the fact that matrix Ca^{2+} modulates GSIS through additional mechanisms that are not directly linked to $[Ca^{2+}]_{cyto}$. These mechanisms might also include the production of mitochondrial coupling factors other than ATP that are responsible for a sustained amplifying phase of GSIS (cf. **1.4**). A recent report supports the latter hypothesis by ruling out that subplasmalemmal Ca^{2+} contributes to the amplifying phase of insulin secretion (105). Tarasov and colleagues, however, recently confirmed the regulatory role of MCU in the glucose-induced generation of ATP (106, 107), which is in agreement with the data presented in **3.5**. In the present study ATP was used as product of OXPHOS and the primary mitochondrial coupling

factor to estimate overall cellular metabolic activity. Other mitochondrial signaling molecules that depend on oxidative metabolism like glutamate or mtGTP (cf. **1.4**) were not assessed. Further studies will be needed in order to identify more mitochondrial coupling factors and their specific contribution to the amplifying phase of GSIS.

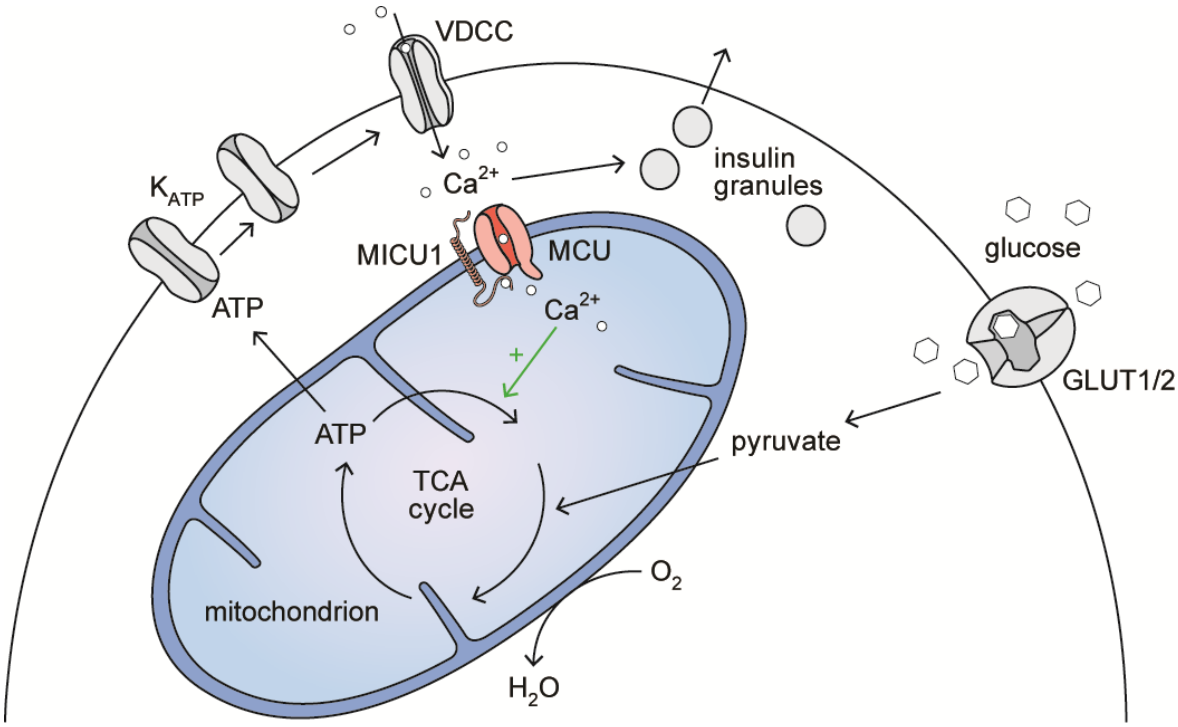

Figure 8. Mitochondrial Ca^{2+} uptake in the pancreatic β-cell. Glucose taken up by the β-cell via glucose transporter 1 or 2 (GLUT1/2) enters glycolysis to yield pyruvate. Pyruvate is transported into the mitochondrion where it fuels the TCA cycle and thereby oxidative metabolism to generate ATP. ATP in turn causes K_{ATP} channels (K_{ATP}) to close triggering Ca^{2+} influx via voltage-dependent Ca^{2+} channels (VDCC). Ca^{2+} entering the cytosol does not only mediate insulin granule exocytosis, but is also transferred to the mitochondrial matrix in a MICU1- and MCU-dependent manner. Matrix free Ca^{2+} activates mitochondrial dehydrogenases and thus acts as a feed-forward mechanism boosting mitochondrial O_2 consumption and the production of ATP and possibly other factors required for a sustained amplifying phase of insulin secretion.

In addition to the striking phenotype on the level of cellular metabolism, cells lacking MICU1 or MCU also showed a pronounced reduction in insulin secretion compared to control cells (**Figure 7**). Coming full circle, **Figure 8** pictures how Ca^{2+} acts at a very late, but also at an early, upstream stage of metabolism-secretion coupling and how MICU1 and MCU contribute to this process.

Considering the fundamental role of mitochondrial Ca^{2+} in regulating cellular metabolic activity, the mitochondrial Ca^{2+} uptake machinery represents a promising therapeutic target for augmenting insulin secretion in type 2 diabetic patients as well as in those patients suffering from subtypes of diabetes associated with mitochondrial dysfunction. Yet, in view of the fact that MCU is a highly conserved and ubiquitously expressed gene (108), the MCU itself is far from being an ideal drug target. Based on the assumption that mitochondrial Ca^{2+} handling is differentially regulated depending on cellular energy status, the source of Ca^{2+} (34) as well as the tissue specific expression pattern of regulatory subunits (90), it might nevertheless be possible to selectively manipulate mitochondrial Ca^{2+} channels and exchangers in β-cells and thereby potentiate GSIS. In order to make proteins such as MICU1 accessible to specific pharmacological interventions, it will be necessary to precisely characterize their molecular interactions and their exact contribution to metabolism-secretion coupling.

REFERENCES

1. Rorsman P, Braun M. Regulation of Insulin Secretion in Human Pancreatic Islets. Annu Rev Physiol. 2012. (in press).
2. Shaw JE, Sicree RA, Zimmet PZ. Global estimates of the prevalence of diabetes for 2010 and 2030. Diabetes Res Clin Pract. 2010 Jan;87(1):4-14.
3. Ashcroft FM, Rorsman P. Diabetes mellitus and the beta cell: the last ten years. Cell. 2012 Mar 16;148(6):1160-71.
4. Zimmet P. The burden of type 2 diabetes: are we doing enough? Diabetes Metab. 2003 Sep;29(4 Pt 2):6S9-18.
5. Ashcroft SJ, Hedeskov CJ, Randle PJ. Glucose metabolism in mouse pancreatic islets. Biochem J. 1970 Jun;118(1):143-54.
6. Wiederkehr A, Wollheim CB. Impact of mitochondrial calcium on the coupling of metabolism to insulin secretion in the pancreatic beta-cell. Cell Calcium. 2008 Jul;44(1):64-76.
7. Henquin JC. Triggering and amplifying pathways of regulation of insulin secretion by glucose. Diabetes. 2000 Nov;49(11):1751-60.
8. Cook DL, Hales CN. Intracellular ATP directly blocks K^+ channels in pancreatic B-cells. Nature. 1984 Sep 20-26;311(5983):271-3.
9. Tarasov A, Dusonchet J, Ashcroft F. Metabolic regulation of the pancreatic beta-cell ATP-sensitive K^+ channel: a pas de deux. Diabetes. 2004 Dec;53 Suppl 3:S113-22.
10. Eliasson L, Abdulkader F, Braun M, Galvanovskis J, Hoppa MB, Rorsman P. Novel aspects of the molecular mechanisms controlling insulin secretion. The Journal of Physiology. 2008;586(14):3313-24.
11. Wiederkehr A, Wollheim CB. Mitochondrial signals drive insulin secretion in the pancreatic beta-cell. Mol Cell Endocrinol. 2012 Apr 28;353(1-2):128-37.
12. Wollheim CB. Beta-cell mitochondria in the regulation of insulin secretion: a new culprit in type II diabetes. Diabetologia. 2000 Mar;43(3):265-77.
13. Waldeck-Weiermair M, Alam MR, Khan MJ, Deak AT, Vishnu N, Karsten F, et al. Spatiotemporal correlations between cytosolic and mitochondrial Ca^{2+} signals using a novel red-shifted mitochondrial targeted cameleon. PLoS One. 2012;7(9):e45917.
14. Tarasov AI, Griffiths EJ, Rutter GA. Regulation of ATP production by mitochondrial Ca^{2+}. Cell Calcium. 2012 Jul;52(1):28-35.
15. Skelin M, Rupnik M, Cencic A. Pancreatic beta cell lines and their applications in diabetes mellitus research. ALTEX. 2010;27(2):105-13.
16. Hohmeier HE, Mulder H, Chen G, Henkel-Rieger R, Prentki M, Newgard CB. Isolation of INS-1-derived cell lines with robust ATP-sensitive K^+ channel-dependent and -independent glucose-stimulated insulin secretion. Diabetes. 2000 Mar;49(3):424-30.
17. Soejima A, Inoue K, Takai D, Kaneko M, Ishihara H, Oka Y, et al. Mitochondrial DNA is required for regulation of glucose-stimulated insulin secretion in a mouse pancreatic beta cell line, MIN6. J Biol Chem. 1996 Oct 18;271(42):26194-9.
18. Tsuruzoe K, Araki E, Furukawa N, Shirotani T, Matsumoto K, Kaneko K, et al. Creation and characterization of a mitochondrial DNA-depleted pancreatic beta-cell line: impaired insulin secretion induced by glucose, leucine, and sulfonylureas. Diabetes. 1998 Apr;47(4):621-31.
19. Kennedy ED, Maechler P, Wollheim CB. Effects of depletion of mitochondrial DNA in metabolism secretion coupling in INS-1 cells. Diabetes. 1998 Mar;47(3):374-80.
20. Pongratz RL, Kibbey RG, Kirkpatrick CL, Zhao X, Pontoglio M, Yaniv M, et al. Mitochondrial dysfunction contributes to impaired insulin secretion in INS-1 cells with dominant-negative mutations of HNF-1alpha and in HNF-1alpha-deficient islets. J Biol Chem. 2009 Jun 19;284(25):16808-21.

21. Silva JP, Kohler M, Graff C, Oldfors A, Magnuson MA, Berggren PO, et al. Impaired insulin secretion and beta-cell loss in tissue-specific knockout mice with mitochondrial diabetes. Nat Genet. 2000 Nov;26(3):336-40.
22. Kadowaki T, Kadowaki H, Mori Y, Tobe K, Sakuta R, Suzuki Y, et al. A subtype of diabetes mellitus associated with a mutation of mitochondrial DNA. N Engl J Med. 1994 Apr 7;330(14):962-8.
23. Coughlan MT, Yap FY, Tong DC, Andrikopoulos S, Gasser A, Thallas-Bonke V, et al. Advanced glycation end products are direct modulators of beta-cell function. Diabetes. 2011 Oct;60(10):2523-32.
24. Kiranadi B, Bangham JA, Smith PA. Inhibition of electrical activity in mouse pancreatic beta-cells by the ATP/ADP translocase inhibitor, bongkrekic acid. FEBS Lett. 1991 May 20;283(1):93-6.
25. Nishi Y, Fujimoto S, Sasaki M, Mukai E, Sato H, Sato Y, et al. Role of mitochondrial phosphate carrier in metabolism-secretion coupling in rat insulinoma cell line INS-1. Biochem J. 2011 Apr 15;435(2):421-30.
26. Rustenbeck I, Herrmann C, Grimmsmann T. Energetic requirement of insulin secretion distal to calcium influx. Diabetes. 1997 Aug;46(8):1305-11.
27. Nakazaki M, Kakei M, Ishihara H, Koriyama N, Hashiguchi H, Aso K, et al. Association of upregulated activity of K_{ATP} channels with impaired insulin secretion in UCP1-expressing insulinoma cells. J Physiol. 2002 May 1;540(Pt 3):781-9.
28. Peyot ML, Gray JP, Lamontagne J, Smith PJ, Holz GG, Madiraju SR, et al. Glucagon-like peptide-1 induced signaling and insulin secretion do not drive fuel and energy metabolism in primary rodent pancreatic beta-cells. PLoS One. 2009;4(7):e6221.
29. Maechler P, Wollheim CB. Mitochondrial function in normal and diabetic beta-cells. Nature. 2001 Dec 13;414(6865):807-12.
30. Groschner LN, Waldeck-Weiermair M, Malli R, Graier WF. Endothelial mitochondria--less respiration, more integration. Pflugers Arch. 2012 Jul;464(1):63-76.
31. Benard G, Bellance N, James D, Parrone P, Fernandez H, Letellier T, et al. Mitochondrial bioenergetics and structural network organization. J Cell Sci. 2007 Mar 1;120(Pt 5):838-48.
32. Park KS, Wiederkehr A, Kirkpatrick C, Mattenberger Y, Martinou JC, Marchetti P, et al. Selective actions of mitochondrial fission/fusion genes on metabolism-secretion coupling in insulin-releasing cells. J Biol Chem. 2008 Nov 28;283(48):33347-56.
33. Twig G, Elorza A, Molina AJ, Mohamed H, Wikstrom JD, Walzer G, et al. Fission and selective fusion govern mitochondrial segregation and elimination by autophagy. EMBO J. 2008 Jan 23;27(2):433-46.
34. Alam MR, Groschner LN, Parichatikanond W, Kuo L, Bondarenko AI, Rost R, et al. Mitochondrial Ca^{2+} uptake 1 (MICU1) and mitochondrial Ca^{2+} uniporter (MCU) contribute to metabolism-secretion coupling in clonal pancreatic beta-cells. J Biol Chem. 2012 Oct 5;287(41):34445-54.
35. Saotome M, Safiulina D, Szabadkai G, Das S, Fransson A, Aspenstrom P, et al. Bidirectional Ca^{2+}-dependent control of mitochondrial dynamics by the Miro GTPase. Proc Natl Acad Sci U S A. 2008 Dec 30;105(52):20728-33.
36. Kennedy HJ, Pouli AE, Ainscow EK, Jouaville LS, Rizzuto R, Rutter GA. Glucose generates sub-plasma membrane ATP microdomains in single islet beta-cells. Potential role for strategically located mitochondria. J Biol Chem. 1999 May 7;274(19):13281-91.
37. Jitrapakdee S, Wutthisathapornchai A, Wallace JC, MacDonald MJ. Regulation of insulin secretion: role of mitochondrial signalling. Diabetologia. 2010;53(6):1019-32.
38. Schuit F, Van Lommel L, Granvik M, Goyvaerts L, de Faudeur G, Schraenen A, et al. Beta-cell-specific gene repression: a mechanism to protect against inappropriate or maladjusted insulin secretion? Diabetes. 2012 May;61(5):969-75.
39. Sekine N, Cirulli V, Regazzi R, Brown LJ, Gine E, Tamarit-Rodriguez J, et al. Low lactate dehydrogenase and high mitochondrial glycerol phosphate dehydrogenase in pancreatic beta-cells. Potential role in nutrient sensing. J Biol Chem. 1994 Feb 18;269(7):4895-902.
40. Mertz RJ, Worley JF, Spencer B, Johnson JH, Dukes ID. Activation of stimulus-secretion coupling in pancreatic beta-cells by specific products of glucose metabolism. Evidence for privileged signaling by glycolysis. J Biol Chem. 1996 Mar 1;271(9):4838-45.

41. Goehring I, Gerencser AA, Schmidt S, Brand MD, Mulder H, Nicholls DG. Plasma membrane potential oscillations in insulin secreting Ins-1 832/13 cells do not require glycolysis and are not initiated by fluctuations in mitochondrial bioenergetics. J Biol Chem. 2012 May 4;287(19):15706-17.
42. Otonkoski T, Jiao H, Kaminen-Ahola N, Tapia-Paez I, Ullah MS, Parton LE, et al. Physical exercise-induced hypoglycemia caused by failed silencing of monocarboxylate transporter 1 in pancreatic beta cells. Am J Hum Genet. 2007 Sep;81(3):467-74.
43. Pullen TJ, Sylow L, Sun G, Halestrap AP, Richter EA, Rutter GA. Overexpression of monocarboxylate transporter-1 (SLC16A1) in mouse pancreatic beta-cells leads to relative hyperinsulinism during exercise. Diabetes. 2012 Jul;61(7):1719-25.
44. Lu D, Mulder H, Zhao P, Burgess SC, Jensen MV, Kamzolova S, et al. 13C NMR isotopomer analysis reveals a connection between pyruvate cycling and glucose-stimulated insulin secretion (GSIS). Proc Natl Acad Sci U S A. 2002 Mar 5;99(5):2708-13.
45. Bricker DK, Taylor EB, Schell JC, Orsak T, Boutron A, Chen YC, et al. A mitochondrial pyruvate carrier required for pyruvate uptake in yeast, Drosophila, and humans. Science. 2012 Jul 6;337(6090):96-100.
46. Herzig S, Raemy E, Montessuit S, Veuthey JL, Zamboni N, Westermann B, et al. Identification and functional expression of the mitochondrial pyruvate carrier. Science. 2012 Jul 6;337(6090):93-6.
47. Malmgren S, Nicholls DG, Taneera J, Bacos K, Koeck T, Tamaddon A, et al. Tight coupling between glucose and mitochondrial metabolism in clonal beta-cells is required for robust insulin secretion. J Biol Chem. 2009 Nov 20;284(47):32395-404.
48. Eto K, Tsubamoto Y, Terauchi Y, Sugiyama T, Kishimoto T, Takahashi N, et al. Role of NADH shuttle system in glucose-induced activation of mitochondrial metabolism and insulin secretion. Science. 1999 Feb 12;283(5404):981-5.
49. Koziel A, Woyda-Ploszczyca A, Kicinska A, Jarmuszkiewicz W. The influence of high glucose on the aerobic metabolism of endothelial EA.hy926 cells. Pflugers Arch. 2012 Dec;464(6):657-69.
50. Nelson DL, Cox MM. Lehninger Principles of Biochemistry. Fifth ed.: W. H. Freeman and Company; 2008.
51. Maechler P, Wollheim CB. Mitochondrial glutamate acts as a messenger in glucose-induced insulin exocytosis. Nature. 1999 Dec 9;402(6762):685-9.
52. Bertrand G, Ishiyama N, Nenquin M, Ravier MA, Henquin JC. The elevation of glutamate content and the amplification of insulin secretion in glucose-stimulated pancreatic islets are not causally related. J Biol Chem. 2002 Sep 6;277(36):32883-91.
53. Hoy M, Maechler P, Efanov AM, Wollheim CB, Berggren PO, Gromada J. Increase in cellular glutamate levels stimulates exocytosis in pancreatic beta-cells. FEBS Lett. 2002 Nov 6;531(2):199-203.
54. Carobbio S, Frigerio F, Rubi B, Vetterli L, Bloksgaard M, Gjinovci A, et al. Deletion of glutamate dehydrogenase in beta-cells abolishes part of the insulin secretory response not required for glucose homeostasis. J Biol Chem. 2009 Jan 9;284(2):921-9.
55. Casimir M, Lasorsa FM, Rubi B, Caille D, Palmieri F, Meda P, et al. Mitochondrial glutamate carrier GC1 as a newly identified player in the control of glucose-stimulated insulin secretion. J Biol Chem. 2009 Sep 11;284(37):25004-14.
56. Kibbey RG, Pongratz RL, Romanelli AJ, Wollheim CB, Cline GW, Shulman GI. Mitochondrial GTP regulates glucose-stimulated insulin secretion. Cell Metab. 2007 Apr;5(4):253-64.
57. Stark R, Pasquel F, Turcu A, Pongratz RL, Roden M, Cline GW, et al. Phosphoenolpyruvate cycling via mitochondrial phosphoenolpyruvate carboxykinase links anaplerosis and mitochondrial GTP with insulin secretion. J Biol Chem. 2009 Sep 25;284(39):26578-90.
58. Akhmedov D, Braun M, Mataki C, Park KS, Pozzan T, Schoonjans K, et al. Mitochondrial matrix pH controls oxidative phosphorylation and metabolism-secretion coupling in INS-1E clonal beta cells. FASEB J. 2010 Nov;24(11):4613-26.
59. Wiederkehr A, Szanda G, Akhmedov D, Mataki C, Heizmann CW, Schoonjans K, et al. Mitochondrial matrix calcium is an activating signal for hormone secretion. Cell Metab. 2011 May 4;13(5):601-11.

60. Boucher BJ, Mannan N, Noonan K, Hales CN, Evans SJ. Glucose intolerance and impairment of insulin secretion in relation to vitamin D deficiency in east London Asians. Diabetologia. 1995 Oct;38(10):1239-45.
61. Gauthier BR, Wollheim CB. Synaptotagmins bind calcium to release insulin. Am J Physiol Endocrinol Metab. 2008 Dec;295(6):E1279-86.
62. Vikman J, Ma X, Hockerman GH, Rorsman P, Eliasson L. Antibody inhibition of synaptosomal protein of 25 kDa (SNAP-25) and syntaxin 1 reduces rapid exocytosis in insulin-secreting cells. J Mol Endocrinol. 2006 Jun;36(3):503-15.
63. Rorsman P, Braun M, Zhang Q. Regulation of calcium in pancreatic alpha- and beta-cells in health and disease. Cell Calcium. 2012 Mar-Apr;51(3-4):300-8.
64. Rojas E, Carroll PB, Ricordi C, Boschero AC, Stojilkovic SS, Atwater I. Control of cytosolic free calcium in cultured human pancreatic beta-cells occurs by external calcium-dependent and independent mechanisms. Endocrinology. 1994 Apr;134(4):1771-81.
65. Hoppa MB, Collins S, Ramracheya R, Hodson L, Amisten S, Zhang Q, et al. Chronic palmitate exposure inhibits insulin secretion by dissociation of Ca^{2+} channels from secretory granules. Cell Metab. 2009 Dec;10(6):455-65.
66. Rutter GA, Tsuboi T, Ravier MA. Ca^{2+} microdomains and the control of insulin secretion. Cell Calcium. 2006 Nov-Dec;40(5-6):539-51.
67. Berridge MJ, Lipp P, Bootman MD. The versatility and universality of calcium signalling. Nat Rev Mol Cell Biol. 2000 Oct;1(1):11-21.
68. Kindmark H, Kohler M, Brown G, Branstrom R, Larsson O, Berggren PO. Glucose-induced oscillations in cytoplasmic free Ca^{2+} concentration precede oscillations in mitochondrial membrane potential in the pancreatic beta-cell. J Biol Chem. 2001 Sep 14;276(37):34530-6.
69. McCormack JG, Halestrap AP, Denton RM. Role of calcium ions in regulation of mammalian intramitochondrial metabolism. Physiol Rev. 1990 Apr;70(2):391-425.
70. Magnus G, Keizer J. Model of beta-cell mitochondrial calcium handling and electrical activity. II. Mitochondrial variables. Am J Physiol. 1998 Apr;274(4 Pt 1):C1174-84.
71. Magnus G, Keizer J. Model of beta-cell mitochondrial calcium handling and electrical activity. I. Cytoplasmic variables. Am J Physiol. 1998 Apr;274(4 Pt 1):C1158-73.
72. Bernardi P, Rasola A. Calcium and cell death: the mitochondrial connection. Subcell Biochem. 2007;45:481-506.
73. Hajnoczky G, Robb-Gaspers LD, Seitz MB, Thomas AP. Decoding of cytosolic calcium oscillations in the mitochondria. Cell. 1995 Aug 11;82(3):415-24.
74. Denton RM, McCormack JG. The calcium sensitive dehydrogenases of vertebrate mitochondria. Cell Calcium. 1986 Dec;7(5-6):377-86.
75. Denton RM, Randle PJ, Martin BR. Stimulation by calcium ions of pyruvate dehydrogenase phosphate phosphatase. Biochem J. 1972 Jun;128(1):161-3.
76. Denton RM, Richards DA, Chin JG. Calcium ions and the regulation of NAD^+-linked isocitrate dehydrogenase from the mitochondria of rat heart and other tissues. Biochem J. 1978 Dec 15;176(3):899-906.
77. McCormack JG, Denton RM. The effects of calcium ions and adenine nucleotides on the activity of pig heart 2-oxoglutarate dehydrogenase complex. Biochem J. 1979 Jun 15;180(3):533-44.
78. Boerries M, Most P, Gledhill JR, Walker JE, Katus HA, Koch WJ, et al. Ca^{2+} -dependent interaction of S100A1 with F1-ATPase leads to an increased ATP content in cardiomyocytes. Mol Cell Biol. 2007 Jun;27(12):4365-73.
79. Wernette ME, Ochs RS, Lardy HA. Ca^{2+} stimulation of rat liver mitochondrial glycerophosphate dehydrogenase. J Biol Chem. 1981 Dec 25;256(24):12767-71.
80. Ostenson CG, Abdel-Halim SM, Rasschaert J, Malaisse-Lagae F, Meuris S, Sener A, et al. Deficient activity of FAD-linked glycerophosphate dehydrogenase in islets of GK rats. Diabetologia. 1993 Aug;36(8):722-6.

81. Jouaville LS, Pinton P, Bastianutto C, Rutter GA, Rizzuto R. Regulation of mitochondrial ATP synthesis by calcium: evidence for a long-term metabolic priming. Proc Natl Acad Sci U S A. 1999 Nov 23;96(24):13807-12.
82. Ainscow EK, Rutter GA. Mitochondrial priming modifies Ca^{2+} oscillations and insulin secretion in pancreatic islets. Biochem J. 2001 Jan 15;353(Pt 2):175-80.
83. Deluca HF, Engstrom GW. Calcium uptake by rat kidney mitochondria. Proc Natl Acad Sci U S A. 1961 Nov 15;47:1744-50.
84. Beutner G, Sharma VK, Giovannucci DR, Yule DI, Sheu SS. Identification of a ryanodine receptor in rat heart mitochondria. J Biol Chem. 2001 Jun 15;276(24):21482-8.
85. Trenker M, Malli R, Fertschai I, Levak-Frank S, Graier WF. Uncoupling proteins 2 and 3 are fundamental for mitochondrial Ca^{2+} uniport. Nat Cell Biol. 2007 Apr;9(4):445-52.
86. De Stefani D, Raffaello A, Teardo E, Szabo I, Rizzuto R. A forty-kilodalton protein of the inner membrane is the mitochondrial calcium uniporter. Nature. 2011 Aug 18;476(7360):336-40.
87. Baughman JM, Perocchi F, Girgis HS, Plovanich M, Belcher-Timme CA, Sancak Y, et al. Integrative genomics identifies MCU as an essential component of the mitochondrial calcium uniporter. Nature. 2011 Aug 18;476(7360):341-5.
88. Perocchi F, Gohil VM, Girgis HS, Bao XR, McCombs JE, Palmer AE, et al. MICU1 encodes a mitochondrial EF hand protein required for Ca^{2+} uptake. Nature. 2010 Sep 16;467(7313):291-6.
89. Mallilankaraman K, Doonan P, Cardenas C, Chandramoorthy HC, Muller M, Miller R, et al. MICU1 is an essential gatekeeper for MCU-mediated mitochondrial Ca^{2+} uptake that regulates cell survival. Cell. 2012 Oct 26;151(3):630-44.
90. Plovanich M, Bogorad RL, Sancak Y, Kamer KJ, Strittmatter L, Li AA, et al. MICU2, a Paralog of MICU1, Resides within the Mitochondrial Uniporter Complex to Regulate Calcium Handling. PLoS One. 2013;8(2):e55785.
91. Mallilankaraman K, Cardenas C, Doonan PJ, Chandramoorthy HC, Irrinki KM, Golenar T, et al. MCUR1 is an essential component of mitochondrial Ca^{2+} uptake that regulates cellular metabolism. Nat Cell Biol. 2012 Dec;14(12):1336-43.
92. Waldeck-Weiermair M, Duan X, Naghdi S, Khan MJ, Trenker M, Malli R, et al. Uncoupling protein 3 adjusts mitochondrial Ca^{2+} uptake to high and low Ca^{2+} signals. Cell Calcium. 2010 Nov;48(5):288-301.
93. Waldeck-Weiermair M, Malli R, Naghdi S, Trenker M, Kahn MJ, Graier WF. The contribution of UCP2 and UCP3 to mitochondrial Ca^{2+} uptake is differentially determined by the source of supplied Ca^{2+}. Cell Calcium. 2010 May;47(5):433-40.
94. Jiang D, Zhao L, Clapham DE. Genome-wide RNAi screen identifies Letm1 as a mitochondrial Ca^{2+}/H^{+} antiporter. Science. 2009 Oct 2;326(5949):144-7.
95. Waldeck-Weiermair M, Jean-Quartier C, Rost R, Khan MJ, Vishnu N, Bondarenko AI, et al. Leucine zipper EF hand-containing transmembrane protein 1 (Letm1) and uncoupling proteins 2 and 3 (UCP2/3) contribute to two distinct mitochondrial Ca^{2+} uptake pathways. J Biol Chem. 2011 Aug 12;286(32):28444-55.
96. Bondarenko AI, Jean-Quartier C, Malli R, Graier WF. Characterization of distinct single-channel properties of Ca^{2+} inward currents in mitochondria. Pflugers Arch. 2013 (in press).
97. Jean-Quartier C, Bondarenko AI, Alam MR, Trenker M, Waldeck-Weiermair M, Malli R, et al. Studying mitochondrial Ca^{2+} uptake - a revisit. Mol Cell Endocrinol. 2012 Apr 28;353(1-2):114-27.
98. Alam MR. Mitochondrial Ca^{2+} homeostasis and its contribution to metabolism-secretion coupling in pancreatic ß-cells [Dissertation]: Medical University of Graz; 2013.
99. De Marinis YZ, Salehi A, Ward CE, Zhang Q, Abdulkader F, Bengtsson M, et al. GLP-1 inhibits and adrenaline stimulates glucagon release by differential modulation of N- and L-type Ca^{2+} channel-dependent exocytosis. Cell Metab. 2010 Jun 9;11(6):543-53.
100. Palty R, Silverman WF, Hershfinkel M, Caporale T, Sensi SL, Parnis J, et al. NCLX is an essential component of mitochondrial Na^{+}/Ca^{2+} exchange. Proc Natl Acad Sci U S A. 2010 Jan 5;107(1):436-41.

101. Malli R, Frieden M, Osibow K, Zoratti C, Mayer M, Demaurex N, et al. Sustained Ca^{2+} transfer across mitochondria is Essential for mitochondrial Ca^{2+} buffering, sore-operated Ca^{2+} entry, and Ca^{2+} store refilling. J Biol Chem. 2003 Nov 7;278(45):44769-79.
102. Lee B, Miles PD, Vargas L, Luan P, Glasco S, Kushnareva Y, et al. Inhibition of mitochondrial Na^{+}-Ca^{2+} exchanger increases mitochondrial metabolism and potentiates glucose-stimulated insulin secretion in rat pancreatic islets. Diabetes. 2003 Apr;52(4):965-73.
103. Gauthier BR, Wiederkehr A, Baquie M, Dai C, Powers AC, Kerr-Conte J, et al. PDX1 deficiency causes mitochondrial dysfunction and defective insulin secretion through TFAM suppression. Cell Metab. 2009 Aug;10(2):110-8.
104. Forbes JM, Ke BX, Nguyen TV, Henstridge DC, Penfold SA, Laskowski A, et al. Deficiency in mitochondrial complex I activity due to Ndufs6 gene trap insertion induces renal disease. Antioxid Redox Signal. 2013 (in press).
105. Ravier MA, Cheng-Xue R, Palmer AE, Henquin JC, Gilon P. Subplasmalemmal Ca^{2+} measurements in mouse pancreatic beta cells support the existence of an amplifying effect of glucose on insulin secretion. Diabetologia. 2010 Sep;53(9):1947-57.
106. Tarasov AI, Semplici F, Ravier MA, Bellomo EA, Pullen TJ, Gilon P, et al. The mitochondrial Ca^{2+} uniporter MCU is essential for glucose-induced ATP increases in pancreatic beta-cells. PLoS One. 2012;7(7):e39722.
107. Tarasov AI, Semplici F, Li D, Rizzuto R, Ravier MA, Gilon P, et al. Frequency-dependent mitochondrial Ca^{2+} accumulation regulates ATP synthesis in pancreatic beta cells. Pflugers Arch. 2012 Nov 14.
108. Bick AG, Calvo SE, Mootha VK. Evolutionary diversity of the mitochondrial calcium uniporter. Science. 2012 May 18;336(6083):886.